



Final Report

A Study of Panel Zone of Steel Moment Connections Subjected to Earthquake Load

by

Arnon Wongkaew
Department of Civil Engineering
Burapha University
Chonburi, 20131

Contract number: MRG 47802200

Final Report

A Study of Panel Zone of Steel Moment Connections Subjected to Earthquake Load

by

Arnon Wongkaew
Department of Civil Engineering
Burapha University
Chonburi, 20131

Financial support: Commission on Higher Education and Thailand Research Fund

ABSTRACT

A Study of Panel Zone of Steel Moment Connections Subjected to Earthquake Load

by

Arnon Wongkaew

Prior to the 1994 Northridge earthquake, structural engineers in the United States believed that welded steel moment-resisting frame building would provide outstanding performance in earthquakes, exhibiting ductile behavior and resisting very strong ground motions without substantial degradation of its structural capacity. However, the discovery of brittle fracture damage in many steel moment frame buildings after the earthquake revealed substantial misunderstanding the ways engineers previously designed and constructed such steel structures. The common damages came from fractures in the beam-to-column moment connection region. The research presented herein focused on investigating the inelastic performance of unreinforced welded steel moment connection and to identify some potential problems of such a connection by using finite element analysis. First, the finite element model of a typical exterior beam-to-column moment connection subjected to cyclic loading was developed. Then, its analytical results were verified with an available experiment data. Final, guided by the first part, the analytical investigation of panel zone was conducted.

The analytical results show that the state of stresses around the connection area is, in fact, very complex. The current design practice following the classical beam theory is inadequate to meet the required strength of the connections. The beam flanges have to carry a considerable shear force instead of the shear tab. This shear force can cause premature fracture of the beam flanges before they can participate in the inelastic

response. The panel zone study shows that the panel zones demonstrate considerable reserve strength beyond the elastic range without strength degradation of connections. However, an appropriate limit should be assigned in order to get a balanced inelastic response between the panel zone and beam.

Keywords: Exterior Beam-to-Column Moment Connection, Finite Element Analysis, Welded Unreinforced Flanges-Bolted Web Connection, Panel Zone, Shear Force

บทคัดย่อภาษาไทย

การศึกษา PANEL ZONE ของข้อต่อโครงสร้างเหล็กแบบถ่ายโมเมนต์เมื่อรับแรงแผ่นดินใหว อานนท์ วงษ์แก้ว

ก่อนการเกิดแผ่นดินใหวที่เมือง Northridge ในปี 1994 วิศวกรโครงสร้างในประเทศ สหรัฐอเมริกาเชื่อว่า โครงข้อแข็งเหล็กจะแสดงพฤติกรรมที่โดดเด่นในเรื่องความเหนียวและจะสามารถ ต้านทานการสั่นใหวที่รุนแรงได้ โดยไม่สูญเสียความแข็งแรงขององค์อาการโดยรวมหรือสูญเสียน้อย มาก อย่างไรก็ตามหลังการเกิดแผ่นดินไหวที่เมือง Northridge พบว่าโครงข้อแข็งจำนวนมากเกิดรอย แตกร้าวบริเวณรอยต่อระหว่างคาน-เสา และต่อมาพบอีกว่ารอยแตกร้าวเหล่านี้เป็นรอยแตกแบบเปราะ ทำให้วิศวกรส่วนใหญ่มีความกังวล ถึงองค์ความรู้และมาตราฐานในการออกแบบโครงข้อแข็งเหล็กที่ ใช้อยู่ขณะนั้น (ก่อนปี 1994) อาจมีข้อบกพร่องจำเป็นต้องทำการศึกษาเพิ่มเติม จุดมุ่งหมาย เพื่อศึกษาพฤติกรรมข้อต่อคาน-เสาเหล็กและศึกษาปัญหาที่เกิดขึ้นกับโครงสร้างประเภทนี้ เมื่อรับแรงแผ่นดินใหวด้วยวิธีไฟในอิลิเมนต์ โดยเริ่มจากการสร้างแบบจำลองไฟในอิลิเมนต์ของข้อต่อ คาน-เสาชนิด Welded Unreinforced Flanges-Bolted Web: SP4.1 ทำการวิเคราะห์แบบจำลอง SP4.1 และนำผลที่ได้จากการวิเคราะห์เปรียบเทียบกับผลที่ได้จากการทดสอบชิ้นงานจริง จากนั้นจะทำการ ปรับรายละเอียดแบบจำลอง SP4.1 เพื่อทำการศึกษาผลของแผ่น Panel Zone ที่มีต่อโครงข้อแข็ง ผลการ ์ วิเคราะห์แบบจำลอง SP4.1 แสดงให้เห็นว่า แบบจำลองไฟในอิลิเมนต์ที่พัฒนาขึ้นมามีความแม่นยำและ แรงตอบสนองสูงสุดของแบบจำลองมีค่าใกล้เคียงกับค่าที่ได้จากการทดสอบชิ้นงาน ความถกต้องสง และแบบจำลองสามารถแสดงตำแหน่งการครากของข้อต่อได้ตรงกับผลที่ได้จากการทดสอบ

จากการศึกษาพบว่าบริเวณจุดเชื่อมต่อระหว่างปีกคานและหน้าเสานั้นจะเกิดการรวมตัวของ
ความเค้นสูงสุด ซึ่งทำให้บริเวณนี้มีความเสี่ยงในการเกิดรอยแตกสูงที่สุด นอกจากนี้จากการวิเคราะห์
ด้วยโปรแกรมไฟในอิลิเมนต์ยังแสดงให้เห็นว่า การกระจายตัวของความเค้นเฉือนบริเวณจุดเชื่อมต่อ
ระหว่างปีกคานและหน้าเสาไม่เป็นไปตามทฤษฎีของคาน กล่าวคือตามทฤษฎีของคาน ปีกคานด้านบน
และล่างจะรับแรงเฉือนน้อยมาก แต่ผลจากการวิเคราะห์ด้วยวิธีไฟในอิลิเมนต์แสดงว่า ปีกคานทั้ง
ด้านบนและล่างบริเวณรอยเชื่อมต่อนี้จะต้องแบกรับแรงเฉือนที่มีขนาดสูงมาก แทนที่จะเป็นแผ่นเหล็ก
ปะกับรับแรงเฉือน (Shear Tab) ซึ่งแผ่นเหล็กปะกับรับแรงเฉือนนี้ถูกออกแบบไว้สำหรับแรงเฉือน การ

แตกแบบเปราะจึงมีแนวโน้มที่จะเกิดขึ้นที่บริเวณปีกลานนี้สูงมากกว่าบริเวณอื่นๆ และเมื่อเกิดรอยแตก แล้วรอยแตกนี้จะขยายตัวเข้าไปได้ทั้งในปีกเสา หรือขยายตัวเข้าหาแผ่นเอวของลานที่บริเวณช่องเว้น การเชื่อม (Access Hole) จากการศึกษาผลของกระทบของการเกิดการกรากในแผ่น Panel Zone ต่อ พฤติกรรมของข้อต่อพบว่า แผ่น Panel Zone สามารถเกิดการกรากได้มากโดยมิได้แสดงการลดลงของ ค่าความแข็ง (Strength) อย่างไรก็ตามลวรมีการกำหนดระดับการกรากของแผ่น Panel Zone เพื่อให้เกิด การกรากทั้งในแผ่น Panel Zone และในกานแบบลักษณะสมมาตร

คำสำคัญ: ข้อต่อคาน-เสาเหล็กของเสาต้นริม, การวิเคราะห์ด้วยวิธีไฟในอิลิเมนต์, ข้อต่อชนิด Welded Unreinforced Flanges-Bolted Web, แผ่น Panel Zone, แรงเฉือน

ACKNOWLEDGMENTS

This is a final report of a research study financially supported by Commission on Higher Education and the Thailand Research Fund under contract number MRG 47802200. The author is solely responsible for the accuracy of the statements or interpretations contained in this publication. No warranty is offered with regards to the results, findings, and recommendations contained herein, either by Commission on Higher Education or the Thailand Research Fund. These organizations and author do not assume any legal liability or responsibility for the accuracy, completeness, or usefulness of any of the information, product, or processes included in this publication.

TABLE OF CONTENTS

ABSTRACT	i
บทคัดย่อภาษาไทย	iii
ACKNOWLEDGMENTS	v
LIST OF TABLES	viii
LIST OF FIGURES	ix
CHAPTER	
1. INTRODUCTION	1
	nization of the Report2
	OMENT CONNECTIONS AND4
2.2 Review of Related R	esearch4
2.2.1.1 A	ridge Welded Steel Moment Connections5 nalytical Studies of re-Northridge Connections11
2.2.1.2 E	xperimental Studies of re-Northridge Connections12
2.2.3 Studies of 2.2.3.1 D 2.2.3.2 K (1 2.2.3.3 K S 2.2.3.4 E	Panel Zones
3 DEVELOPMENT OF FINIT	FE ELEMENT MODEL27

Introduction	••••••	27
Бреенн	CH D1 1.1	••••••
OF PANEL ZON	ES	47
01 1111 (22 201)	<i></i>	
Panel Zone of an I	Exterior Column	47
4.4.1 Method	ology and Finite Element Models	54
		61
4.4.4 Approp	riate Degree of Yielding in Panel Zones	67
•••••		•••••
ARY AND CONC	LUSIONS	70
	1 .	70
Summary and Cor	nclusions	/ U
. (Finite Element Moverification of Fir Elastic Analysis of 3.5.1 Conclus Specime OF PANEL ZON Panel Zone of an I Panel Zone Design Shear Strength and Analytical Study of 4.4.1 Method 4.4.2 Behavior 4.4.3 Influence the Conclusion of Firence and Conclusion of Firence and Conclusion of Firence and Conclusion of The Conc	4.4.3 Influences of Panel Zone Yielding to the Connection Interface Area

LIST OF TABLES

Table

2.1.	Types of girder damage (FEMA/SAC 1995)	9
	Types of column damage (FEMA/SAC 1995)	
	Types of weld damage (FEMA/SAC 1995)	
	Types of shear tab damage (FEMA/SAC 1995)	
2.5.	Types of panel zone damage (FEMA/SAC 1995)	.11
3.1.	Properties of analysis of specimen SP4.1	.29
3.2.	Coupon yield/ultimate stress data of specimen SP4.1	.29
3.3.	Summary of maximum stress and shear force distributions in the beam flange	.46
4.1.	Properties of analyzed models	
4.2.	Ratios of shear strengths to shear demand of panel zones	.58
4.3.	Comparison of the maximum beam bending moments	.65

LIST OF FIGURES

Figure

2.1.	A typical interior and exterior pre-Northridge
	beam-to-column moment connection
2.2.	Types of connection damage observed after the Northridge earthquake8
2.3.	Post–Northridge connection16
2.4.	Typical details of the reduced beam section connection and
	its hysteretic response
2.5.	A typical details of the free flange connection and its hysteretic response18
2.6.	Other possible connections qualifying as welded fully restrained connection20
3.1.	Location of the exterior connection sub-assembly in a typical steel moment frame
3.2.	a) Drawing of the test set-up at the University of Michigan31
3.2.	b) Photograph of the test set-up at the University of Michigan31
3.3.	Loading history for the University of Michigan specimens
3.4.	S4R: 4 node reduced integration shell element33
3.5.	A finite element model of specimen SP4.135
3.6.	Stress-Strain curve for steel used in the inelastic analysis
3.7.	Comparison of load-displacement responses between test and FEA of SP4.138
3.8.	Shear stress and von Mises stress contours for Specimen SP4.139
3.9.	Principal stress vectors in the connection area41
3.10	von Mises stress distributions in the connection area41

42	3.11. von Mises stress distributions on the beam flange
44	3.12. Shear stress distributions in the shear tab, 0.25 in. from the column face
45	3.13. Shear force distributions in the top half and bottom half of the beam flange
45	3.14. Shear stress (S12) contours in the shear tab
	4.1. Parameters, free-body, shear, and moment diagrams of
75	a typical column in exterior connection specimens
60	4.2. Deformed shapes of model BC1 and BC16
60	4.3. von Mises stress contours in panel zones of model BC1 and BC16
65	1.4. Shear forces carried by shear tabs at the different story drifts
	4.5. Tensile stress distributions on beam flanges at the interface area of
66	1% and 4% story drifts, respectively
	4.6. % shear forces carried by the beam flanges vs. shear strength ratios of
69	the panel zones at approximately 0.5%, 1%, 2%, 4% story drifts

CHAPTER 1 INTRODUCTION

1.1 BACKGROUND

On January 17, 1994, a fairly moderate earthquake, later named the Northridge earthquake, struck a northwestern suburb city, Northridge, of Los Angeles. The Northridge earthquake caused widespread building damages, resulting in estimated economic losses exceeding \$30 billion. Much of the damage sustained was quite predictable, occurring in types of buildings that engineers had previously identified as having low seismic resistance and significant risk of damage in earthquakes. Reinforced and pre-stressed concrete parking garages perhaps were the most problem-prone structures, resulting in total collapse. Yet, considered all the destruction surrounding the area, steel structures stood. There were no deaths associated with steel-framed buildings, no structural collapses and, in general only minor nonstructural damages to steel frames building. However, closer inspection after the earthquake has revealed damage to the beam-to-column connections in over 100 steel-framed buildings in the area. Even though those buildings are considered as modern steel structures, which were designed with the updated design codes.

The steel structures employed in the majority of buildings in Northridge were the special moment resisting frame (SMF). Engineers had believed that SMF would behave in a ductile manner, bending under loading from earthquakes, but not breaking. The common damage consisted of a brittle fracturing of the steel frames at welded joints between beams and columns. The discovery of the potential for fracturing in these frames effectively invalidated the entire portion of the building code dealing with SMF construction and created a crisis of confidence. These connection damages have raised

questions regarding how safe the existing moment resisting frames are, and how new moment resisting frames should be designed, especially the moment connections.

The Federal Emergency Management Agency (FEMA) responded to this crisis by initiating a four year program of research with the SAC Joint Venture to investigate and rapidly develop guidelines to:

- 1) identify, inspect, evaluate, repair or modify damaged welded steel building following a potentially damaging earthquake;
- 2) identify, inspect, evaluate, and retrofit at risk welded steel frame buildings prior to an earthquake, and
- 3) design and construct new steel frame buildings.

The SAC Joint Venture consists of three non-profit professional and educational organizations: the Structural Engineers Association of California (SEAOC), the Applied Technology Council (ATC) and the California Universities for Research in Earthquake Engineering (CUREe). The program actively involved engineers, researches, construction experts and other specialists from throughout the U.S. The project was divided into two major phases. The first phase focused on the development of Interim Guidelines. This effort was achieved in August 1995, with publication of FEMA-267, Interim Guidelines: Inspection, Evaluation, Repair, Modification and Design of Welded Steel Moment Frame Structures (SAC, 1995). The second phase was completed by the end of the year 2000 with publication of FEMA 350-355 reports.

To date, some questions have been answered, but some still remained shrouded in doubts. The purpose of this research is to study the behavior of the welded steel beam-to-column moment connections in respect to the panel zone strength. The study focused on answering: how these elements contribute to the ductility and fracture of the connections, and how they should be designed.

1.2 OBJECTIVES AND ORGANIZATION OF THE REPORT

The research presented in this report was carried out on steel moment connections (a welded unreinforced flanges-bolted web type) under monotonic and cyclic loading

through detailed three-dimensional nonlinear finite element (FE) analyses. The objectives of this research can be described as follows:

- 1) To develop a more through understanding of the inelastic behavior of steel connections
- 2) To investigate the effects of panel zone strength on the ductility and potential for fracture of the steel moment connections
 - 3) To present an idea for the use of balanced panel zone yielding.

This report is organized into 5 chapters. Chapter 1 presents overview of the research, motivation, objectives, and organization of the research. Chapter 2 introduces a review of typical moment connection configurations and their design concepts. The moment connection damages reported by FEMA due to the 1994 Northridge earthquake are also presented herein. In addition, literature review of previous analytical and experimental works on steel moment connections and panel zone is given in this chapter. Chapter 3 includes development of linear and nonlinear finite element (FE) analyses of the steel moment connections. The results of these analyses are used to identify potential problems in the connections. Chapter 4 presents the behavior of the moment connections designed by strong and weak panel zone concepts based on FE analyses. The advantages and disadvantages of such connections are presented and discussed. Chapter 5, the final chapter, presents the summary and concluding remarks of the study. Suggestions for possible future study are also presented.

CHAPTER 2

A REVIEW OF STEEL MOMENT CONNECTIONS AND RELATED RESEARCH

2.1 INTRODUCTION

Primary design procedures for steel moment-resisting structures are to allow basic components such as beams, columns, and panel zones to be able to dissipate hysteretic energy during an earthquake by developing large plastic rotations, without significant loss of the connection strength. Prior to the Northridge earthquake, plastic rotation expected in a beam alone (in the absence of panel zone plastic deformation) was targeted at 0.02 radian (Tsai 1988, Popov and Tsai 1989). However, after the Northridge earthquake, the required connection plastic rotation capacity (beam and panel zone) was increased to 0.03 radian for new construction and 0.025 radian for a post-earthquake retrofitting of existing buildings (SAC 1995).

2.2 REVIEW OF RELATED RESEARCH

Many analytical and experimental studies have been carried out in the past to study the seismic behavior of steel moment connections. These studies ranged from monotonic and cyclic loading tests of the full-scale and reduced-scale moment connections to analytical investigations of the seismic behavior of the moment connections with respect to various connection components. However, to serve the purposes of this research, the study of the literature was focused on major findings related to overall behavior of connections and to those of the panel zone parameter.

2.2.1 Pre-Northridge Welded Steel Moment Connections

Figure 2.1 shows a typical interior and exterior pre-Northridge welded flange-bolted web beam-to-column moment connection, respectively. Beam flanges are welded to the column flange and the beam web is typically connected to the column flange by bolting to a single shear tab, which is itself welded to the column flange. The pre-Northridge moment connection design was initially developed in the late 1960s and early 1970s. It should be noted that the entire shear force is assumed to be carried by the shear tab and the bending moment is transferred to the column flange through the beam flanges. It can be seen that the design criterion is in fact following the assumptions of the classical beam theory. This design criterion has been widely applied to the designs for many years.

According to Uniform Building Code (UBC-94) and AISC-LRFD specification (1995-2005), some other connection details can be added depending on certain prerequisites. For example, supplemental welds of the shear tab are necessary when the flexural strength of the beam flanges is less than 70% of the flexural strength of the entire beam section. If the shear strength of the panel zone is not adequate, either column web doubler plates or diagonal stiffeners should be provided. Continuity plates are recommended to prevent local buckling or local yielding of the column web near the beam flange levels. All these criteria stated by the current design codes were developed approximately in the 1970s-1980s.

It is important to know the types of damage suffered by the moment connections during recent major earthquakes. Then, the improvements can be made in those areas. More than 150 steel moment-resisting frame buildings were identified to have serious damages in beam-to-column connections in the Northridge earthquake. Common types of damage in the welded steel moment connections were found in/or near the beam-column flange welds. Figure 2.2 shows the types of commonly observed beam-to-column

moment connection damage, taken from the FEMA/SAC Interim Guidelines (1995). Descriptions of each damage type are provided in Table 2.1 through 2.5.

As can be seen, the most common types of damage were beam flange tearing, fracture in the weld material, and fracture in the column flanges. The most serious and undesirable type of damage was fracture of columns. In some cases, fracture in the column flanges penetrated through the column web. It was reported that cracks near the beam bottom flange were more common than the cracks near the beam top flange. These types of fractures, cracking, and tearing were sudden brittle failures with a very limited sign of yielding.

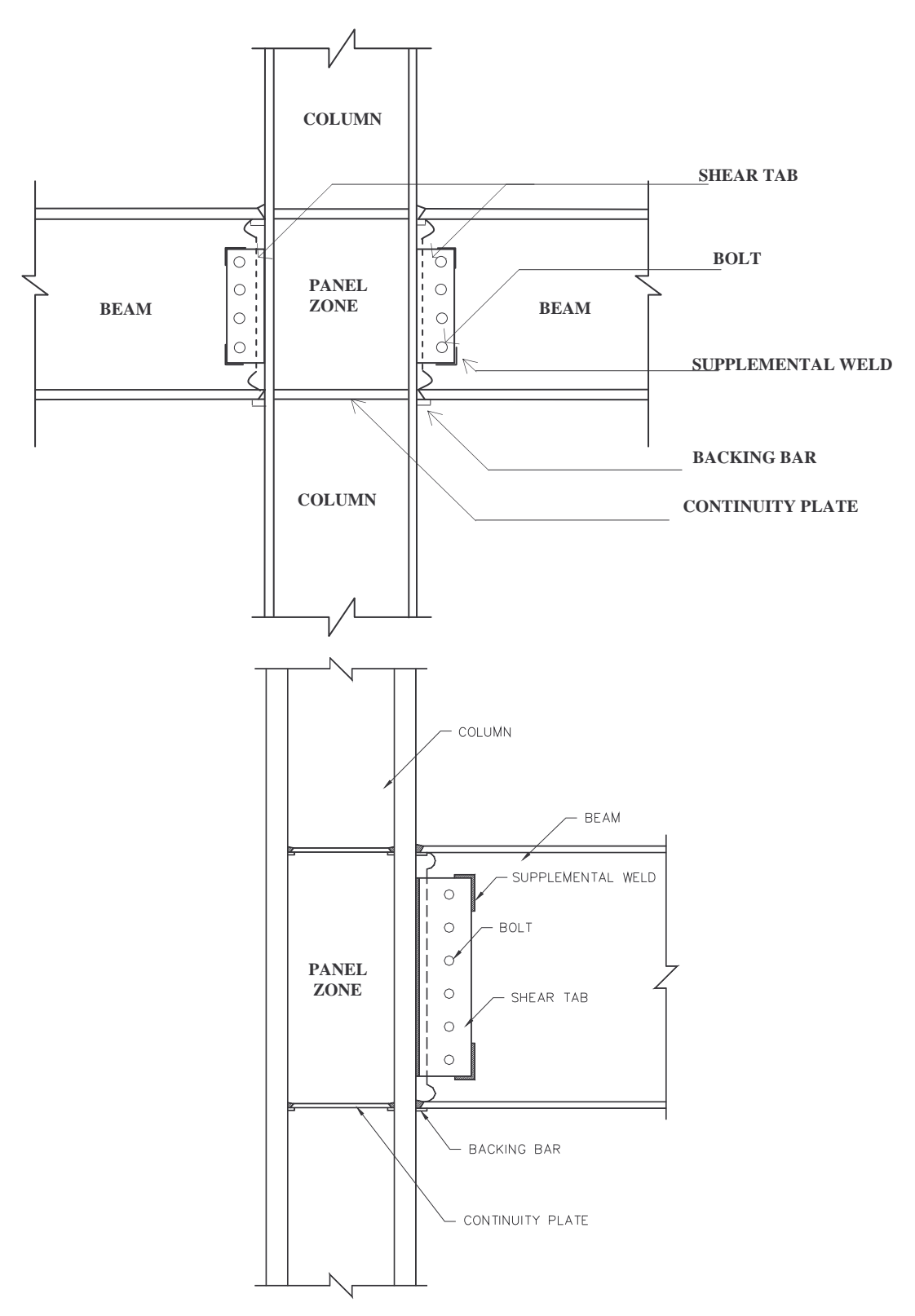


Figure 2.1. A typical interior and exterior pre-Northridge beam-to-column moment connection, respectively [34].

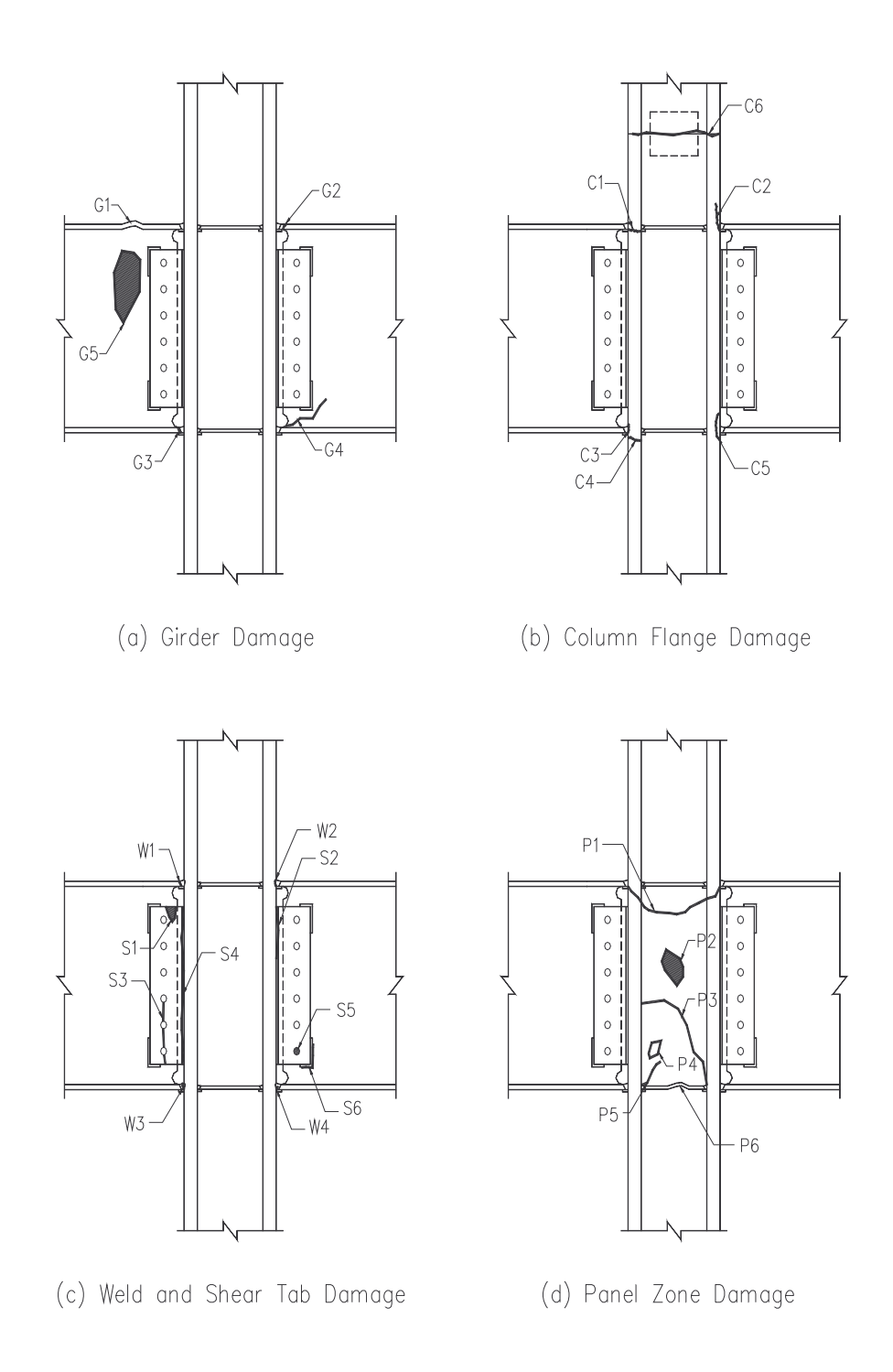


Figure 2.2. Types of connection damage observed after the Northridge earthquake [16].

Table 2.1. Types of girder damage (FEMA/SAC 1995).

Туре	Description
G1	Buckled flange (top or bottom)
G2	Flange tear out near weld (top or bottom)
G3	Flange fracture in heat affected zone (top or bottom)
G4	Fracture of web
G5	Yielding or buckling of web

Table 2.2. Types of column damage (FEMA/SAC 1995).

Type	Description
C1	Incipient flange crack
C2	Lamellar flange tearing
C3	Full or partial flange crack in heat affected zone
C4	Full or partial flange crack outside heat affected zone
C5	Flange tear-out or divot
C6	Column splice failure

Table 2.3. Types of weld damage (FEMA/SAC 1995).

Type	Description
W1	Fracture at girder flange interface
** 1	Tracture at girder mange interface
W2	Fracture at column interface
W3	Crack through weld metal thickness
W4	Incipient crack, especially at weld root

Table 2.4. Types of shear tab damage (FEMA/SAC 1995).

Type	Description
S1	Yielding or buckling of tab
S2	Partial crack at weld to column
S3	Fracture through tab at bolts or severe distortion
S4	Full length fracture of weld to column
S5	Loose, damaged or missing bolts
S6	Fracture of supplemental weld

Table 2.5. Types of panel zone damage (FEMA/SAC 1995).

Type	Description
P1	Severed column
P2	Yielding or ductile deformation of web
Р3	Full or near full depth fracture in web or doubler plate
P4	Full or near full depth fracture in web
P5	Partial depth fracture in doubler plate
P6	Fracture, buckle, or yield of continuity plate

2.2.1.1 Analytical Studies of Pre-Northridge Connections

After the Northridge earthquake, finite element (FE) analysis was used by many researchers as the most common and cost-effective tool to study welded-bolted steel connections. The analyses were conducted using various commercial FE programs such as ABAQUS, ANSYS, NASTRAN, etc. Patel and Chen (1984) studied the inelastic behavior of moment connections, assuming 2-D plane stress behavior and employing von Mises yield criterion in their FE models. The researchers concluded that their FE models were successfully simulating the observed behavior of weld-bolted connections, especially the load-deflection behavior, and stress distributions in panel zones. It should be noted that the study accounted for thermal residual stresses, but geometric imperfections were not included, and the loading type was only monotonic.

Similarly, Yang and Popov (1995) performed 3-D inelastic analyses of connection subassemblages tested as a part of their research using ABAQUS. With 8-node brick elements, von Mises yield criterion, and neglecting residual stresses and geometric imperfections, the models were able to deliver good correlation between the analytically

calculated load-displacement curves and the experimental measured ones. In addition, they also found that the stress intensity factor for the beam bottom-backing bar was larger than that for the beam top-backing bar. They suggested that this could be the reason for large number of beam bottom flange fractures over top flange fractures as discovered in moment-resisting frame (MRF) buildings following the Northridge earthquake.

Goel et al. (1996), based on observations from 3-D elastic FE analyses of shell element models, concluded that the stress distributions at the beam-to-column interface were very complex, with most of the shear force being carried by the beam flanges, and not the beam web as assumed in the classical beam theory. The flow of forces was better described by truss analogy, which was later used as a new design concept for the new high-performance moment connection type.

Chi et al. (1997) conducted a series of 2-D and 3-D linear elastic fracture mechanics and inelastic fracture analyses of pre-Northridge type connections using the programs FRANC and ABAQUS to investigate the phenomenon of fracture beneath the weld backing bar, which dominated the fractures in the connections found in the Northridge earthquake. Their FE analyses concluded that the presence of discontinuities and flaws at the root of the weld was most likely a source for fracture initiation. Moreover, placing a fillet weld at the underside of the connections was susceptible to brittle fracture in the elastic range.

2.2.1.2 Experimental Studies of Pre-Northridge Connections

Prior to the Northridge earthquake, many researchers (Tsai and Popov 1989, Engelhardt and Husain 1993) began to point out potential problems with the welded flange-bolted web moment connections observed from their experiments such as brittle weld fracture and a lack of beam plastic rotations. Despite these reports, designers still remained confident about validity of the welded steel moment-resisting frames under

seismic loading. Their confidence was based on the fact that most of connection test specimens achieved 0.015 radians of total plastic rotation under cyclic loading, which was the generally accepted minimum required plastic rotation capacity (Engelhardt and Husain 1993). This conclusion was drawn from analytical studies of the responses of typical steel MRF buildings to typical earthquake records available at that time, such as the study by Tsai and Popov (1989).

After the 1994 Northridge earthquake, a number of steel moment connections suffered serious damages similar to the failure modes observed in the previous experiments. Then, it was quickly concluded that steel moment frames are not ductile enough to resist intense seismic loading.

There were numerous studies from both academic and industrial sides to investigate and reevaluate various aspects that were believed to be associated with the failures observed in the pre-Northridge connections.

The results from experimental programs sponsored by AISC and SAC Joint Venture immediately after the Northridge earthquake [34, 35, 36] showed that the connections failed abruptly due to beam flange fracture at/or near the welds, which was the common type of connection damage observed in the existing damaged buildings after the earthquake. Most of the tests indicated that only a small amount of yielding and plastic deformation occurred in the beams or the panel zones. The tested specimens consisted of typical beam and column sizes used in practice, ranging in size from W24x68 to W36x150 for beam and W14x120 to W14x257 for column. All the specimens were fabricated by closely following the welding methods used before the Northridge earthquake. The backing bars and weld tabs were left in place.

As concluded in the FEMA/SAC Interim Guidelines [17], the left-in-place backing bars and run-off tabs after welding the flange with complete joint penetration welds can cause the initiation of fracture. Fracture appeared to originate from cracks that developed at the notches in the root of the complete joint penetration flange welds.

Moreover, the weld metals with low toughness (E70-T4), typically employed in the US construction, had inadequate capacity to arrest fracture once it initiated under loading. The other potential factor contributing to brittle fracture was the difference between nominal and actual strength of the US-made steel rolled shapes. Also, the use of relatively weak panel zones, that yielded in shear under the influence of beam flexural demand as allowed by recent editions of the code, can result in the development of additional stress concentrations at the junction beam flanges and the column flanges, further adding to the tendency of fracture initiation.

2.2.2 Post-Northridge Welded Steel Moment Connections

Based on information gathered from the SAC Phase I study, a new design practice for steel moment connections was recommended by SAC Joint Venture in order to improve the overall behavior of the connections. The new details of such connections are shown in Figure 2.3. The new configurations include: the use of notch-tough weld metals with a specified minimum Charpy V-notch toughness of 20 kips-ft at -20°F, the removal of backing bar and run-off tabs from the beam bottom flange after beam flange groove welding, the use of taller shear tabs and more bolts, the use of continuity plates, and the use of a fatigue-resistant geometry of the weld access hole etc.

Ten post-Northridge beam-to-column welded unreinforced flange moment exterior connections using notch tough electrode and with bolted beam web were tested by Goel et al. (1999) under SAC Phase II to investigate their cyclic ductility. The beam size varied from a W24 to W36. The results showed that the typical failure modes of the tested specimens were fracture of either the base metal of the beam flanges or the weld metal. The crack was located in the area between the heat affected zone on the outside flange surface and the tip of the access hole on the inside flange surface. After a crack appeared on the outside surface of the flange, a subsequent crack formed on the inside

surface of the flange, usually in the next displacement cycle, at the tip where the access hole met the flange. During the next increased displacement cycle that followed, both cracks propagated through the flange thickness in the ductile manner, which was the slow fracture of the base metal. Then, crack propagation became unstable, and the entire flange fractured in a brittle manner. Tested specimens had a plastic rotation capacity in the range of 0.01 to 0.026 radian.

From these test results, it was concluded that a moment connection fabricated using high notch-tough electrodes, and with some modifications of the pre-Northridge welded unreinforced flange moment connection details was beneficial, but not qualify for using in special or intermediate moment resisting frames. The current required ductility for SMRFs (special moment resisting frames) and IMRFs (intermediate moment resisting frames) are 0.03 and 0.02 radians of total plastic connection rotation [SAC 1995], respectively.

In addition to the post-Northridge connection, five specimens of the exterior moment connections so called "Free-Flange connection", were tested by Goel et al. (2000) at the University of Michigan, and two additional free-flange connections were tested at the University of Texas and the University of California. The complete design procedures can be found in reference [37]. The specimens had beam sizes varying from a W24 to W36 with the varied column sizes of W14 section. The test results showed a significant improvement in performance. The connections successfully satisfied the minimum required ductility for SMRFs (total plastic rotation of at least 0.03 radians).

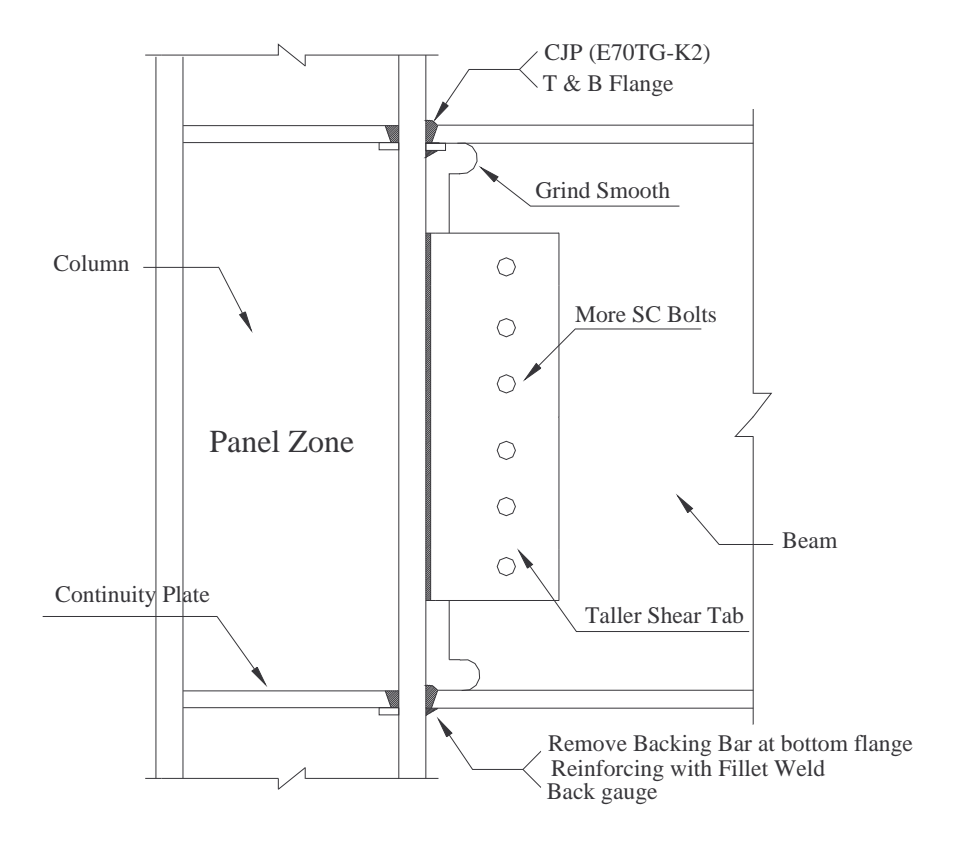


Figure 2.3. Post–Northridge connection [35].

According to AISC Seismic Provision 2005, the qualified moment connections shall be capable of sustaining interstory drifts of at least 0.04, 0.02, and 0.01 radians for Special, Intermediate, and Ordinary Moment Frame (SMF, IMF, and OMF), respectively. Since the elastic drift of typical moment frames is usually in the range of 0.01 radians and the inelastic rotation of the beams is approximately equal to the inelastic drift, therefore SMF and IMF are designed to accommodate inelastic rotations of 0.03, and 0.01 radians, respectively. For this new AISC provision, OMF should be designed to remain essentially elastic and are assumed to have only very small inelastic demand. The new provisions for these three moment-frame types base primarily on lessons learned from the Northridge and Kobe Earthquakes, and benefit from subsequent research performed by the SAC

Joint Venture for FEMA. The reader is referred to FEMA 350 for an extensive discussion of these studies and recommendations.

The prequalified welded fully restrained connection types stated in FEMA 350 can be described as

- 1) Welded Unreinforced Flanges-Bolted Web, qualifying for OMF.
- 2) Welded Unreinforced Flanges-Welded Web, qualifying for OMF and SMF
- 3) Free Flange, qualifying for OMF and SMF
- 4) Reduced Beam Section, qualifying for OMF and SMF
- 5) Welded Flange Plate, qualifying for OMF and SMF

However, only reduced beam section is adopted by AISC 2005 as a prequalified welded fully restrained connections using for IMF and SMF. It should be noted that OMF in FEMA 350 is equivalent to IMF in AISC 2005. Figure 2.4 shows a typical configuration of the reduced beam section connection and its hysteretic response. Figure 2.5 provides a typical detail for the free flange connection and its hysteretic response.

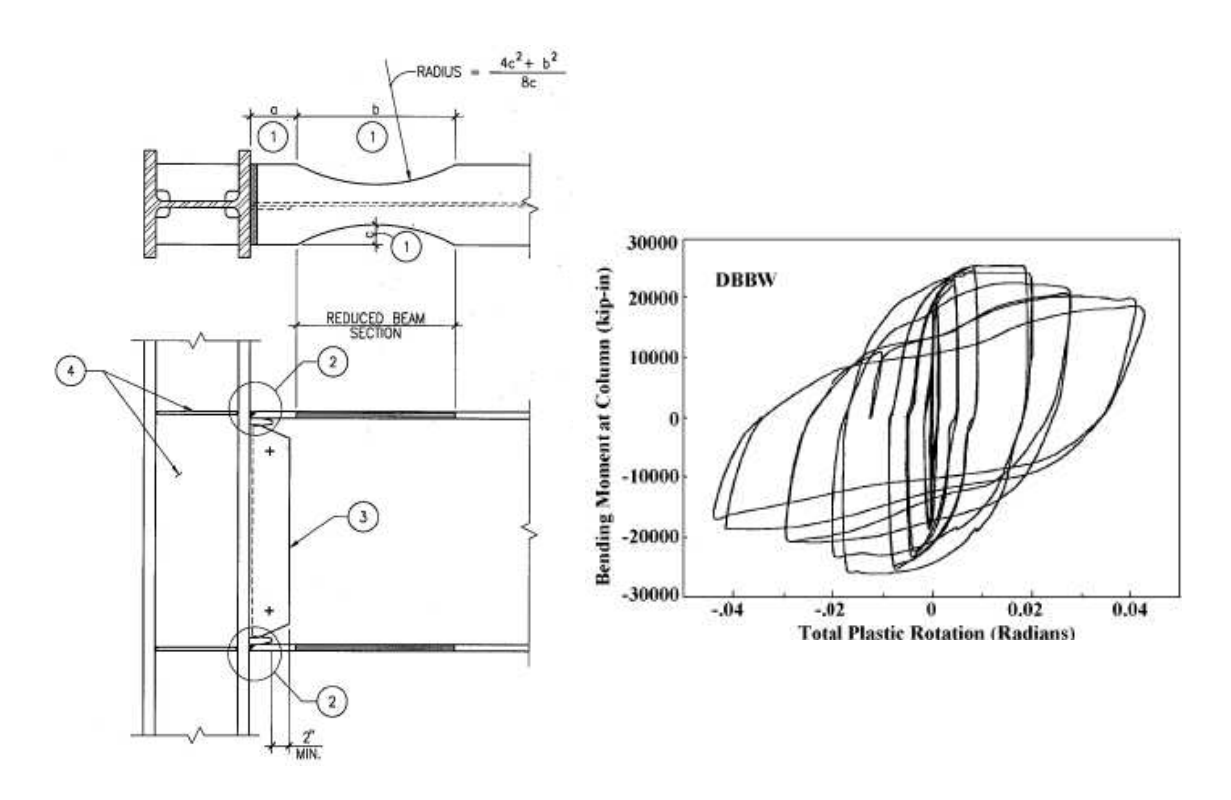


Figure 2.4. Typical details of the reduced beam section connection and its hysteretic response [18].

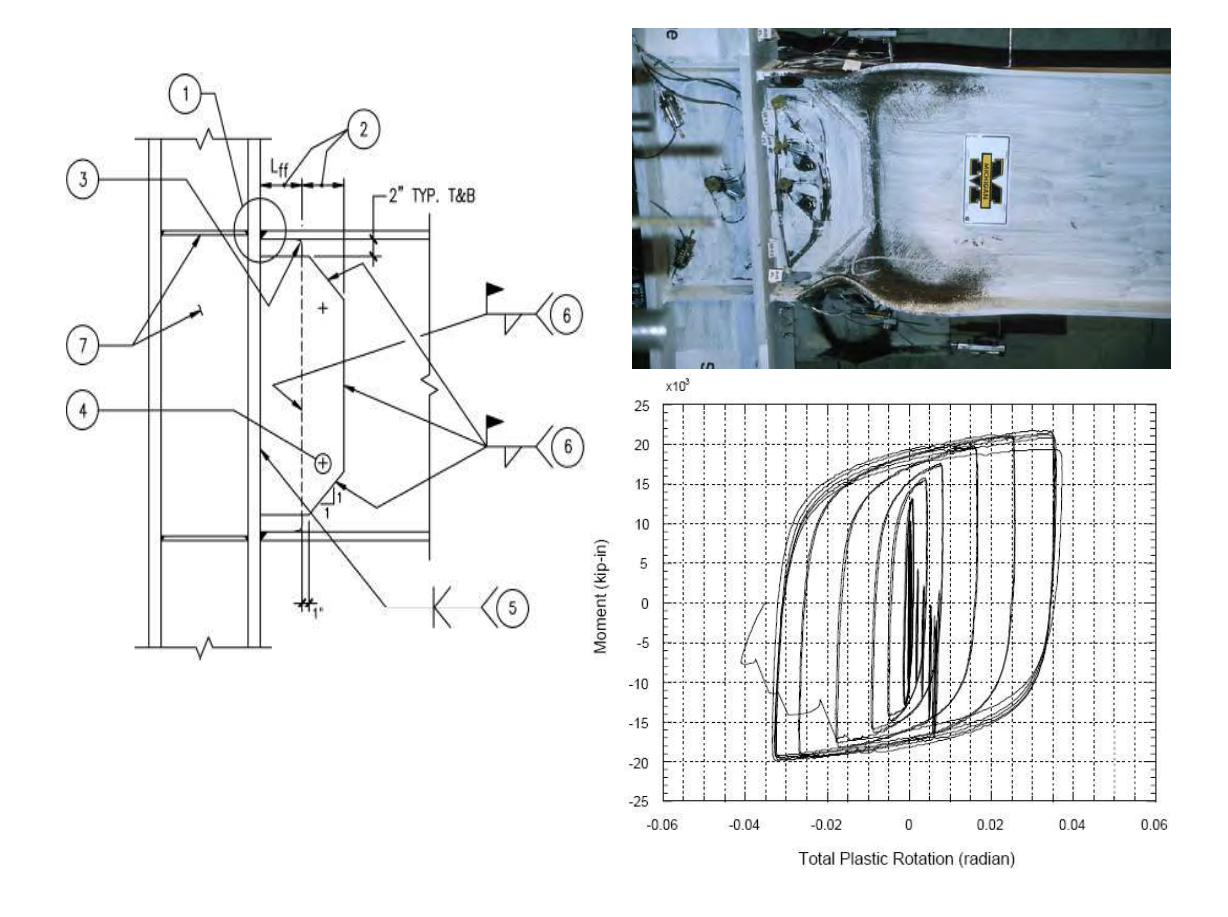
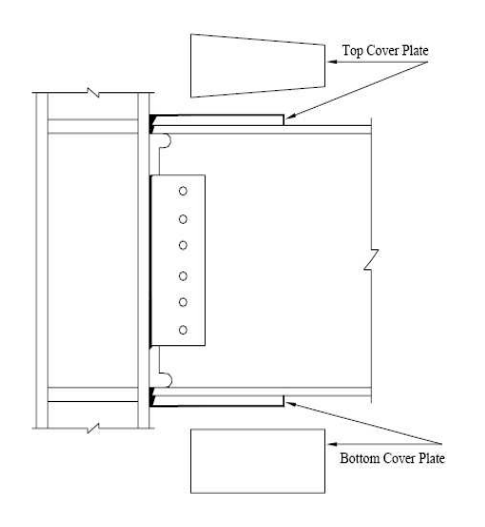


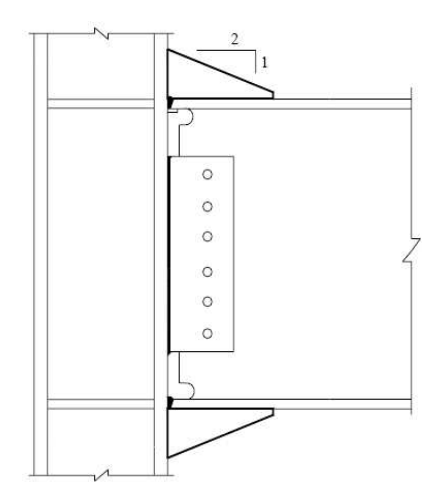
Figure 2.5. A typical details of the free flange connection and its hysteretic response [18].

In addition to those prequalified connection types, there are some connection types for which extensive testing has been performed have not been included as prequalified for new buildings. These include the following:

- 1) Cover Flange Plate Connection
- 2) Flange Rib Connection
- 3) Haunch Connection
- 4) Flange Plate and Vertical Rib Connection
- 5) Side Plate Connection
- 6) Slotted Web Connection

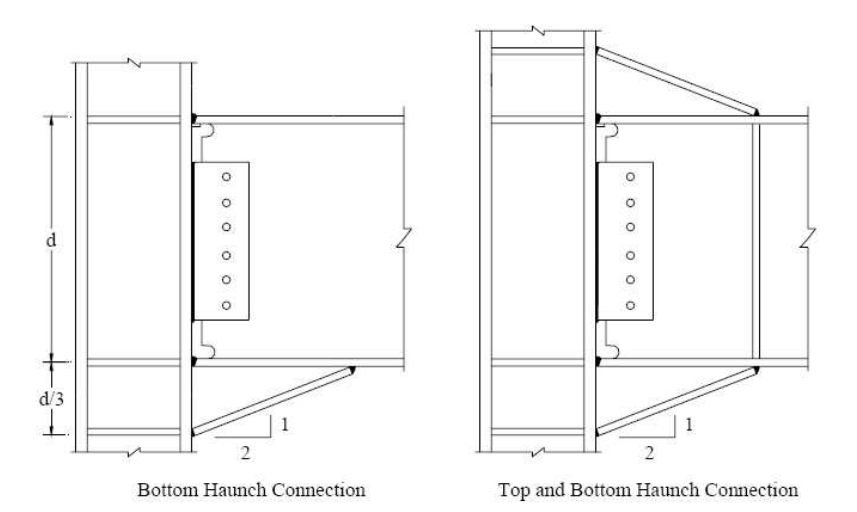
These connections are not included because the tested data for those connection types is insufficient to permit prequalification. Those kinds of connections are shown schematically in Figure 2.6.





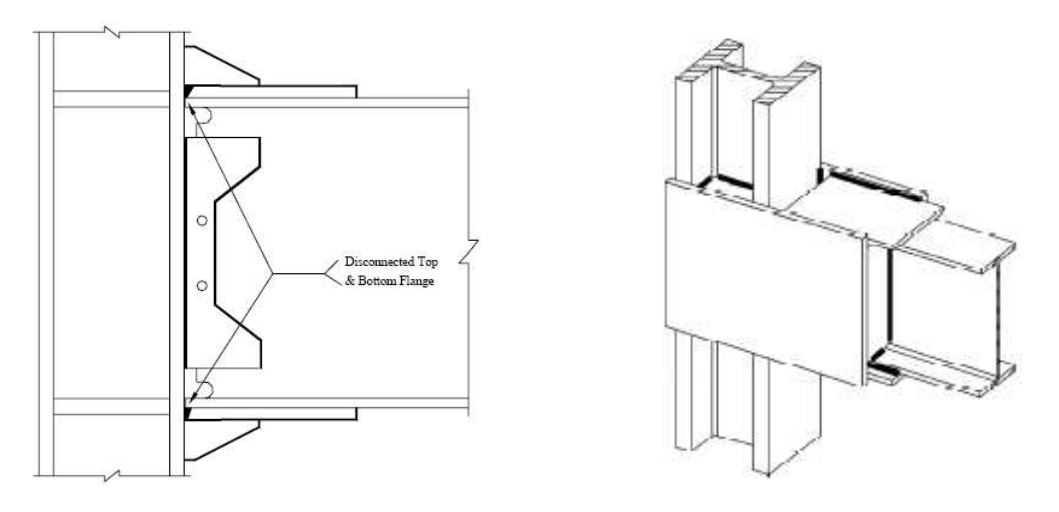
Cover Flange Plate Connection

Flange Rib Connection



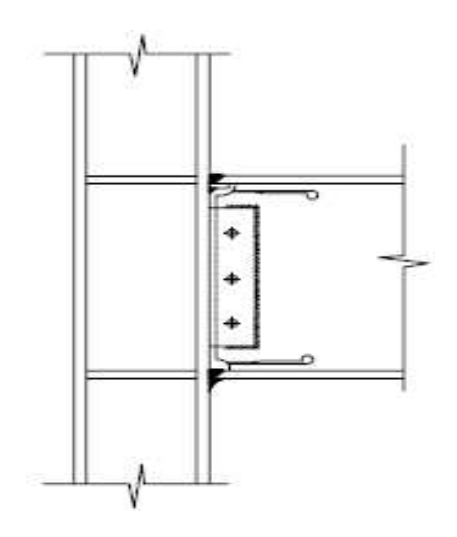
Haunch Connection

[continue]



Flange Plate and Vertical Rib Connection

Side Plate Connecion



Slotted Web Connection

Figure 2.6. Other possible connections qualifying as welded fully restrained connection [18].

2.2.3 Studies of Panel Zones

2.2.3.1 D.J. Fielding and J.S. Huang 1971

The main objective of the research was to study the influence of axial force on the behavior of beam-to-column connections that also carry high shear from the beam moment. The experiment was conducted in order to confirm the previous experiment on seven pilot scale tests of the beam-to-column connections in 1966 (J.W. Perters and G.C. Driscoll Jr.). The specimen consisted of a W14x184 column and a W24x160 beam of ASTM-A36, representing an exterior column and the left-hand portion of a beam from a multistory frame. The specimen was designed to fail in the column web panel before failure in the beam section. The column web panel was designed by using the 1969 AISC design equations, which were based on the simplified plastic design strength of the effective web area. The axial load was initially applied at the top of column up to P/P_y=0.5, and maintained at this force level. After that, the beam was slowly loaded at the end monotonically. The main result was that there was a large margin of the reserve shear strength of the connection, although the column was under a considerable axial load. This was also evident in the previous test with the axial load ratio P/P_y of 0.8. The column web panel was plastified without web buckling or web crippling. The reserve strength varied between factors of 1.25 to 2.75. This suggested that the AISC design formula for panel zones was conservative.

2.2.3.2 Krawinkler, H. and et al. (1971, 1973, 1975, and 1978)

The inelastic behavior of panel zones was intensively studied by Krawinkler et al. in 1970s. The main purposes of their studies were to evaluate the AISC design criteria for joint shear, and to suggest and modify better equations as the design criteria. The study also included the effects of high shear on the beam-to-column joint strength, and on the ductility of the moment-resisting frames. Their experiments on large-scale specimens clearly showed that the panel zones with careful details to avoid column web yielding, buckling, crippling and column flange distortion can exhibit excellent energy dissipation in shear under large inelastic deformations. This showed that the panel zones have considerable reserve strength beyond the first sign of yielding. The additional strength

can largely be attributed to elements surrounding the panel zones, together with strain hardening of the column web in shear. This observation led Krawinkler et al. to propose a simplified mathematical model to compute the ultimate shear strength of the panel zones. The model agreed well with experimental results for joints with thin to medium column flange thickness. However, the suggested model needed to be verified with experiments for the columns with thicker flanges.

The proposed mathematical model consists of an elastic-perfectly plastic column web surrounded by rigid boundaries with four springs at the corners. These springs represent the bending resistance of the column flanges at the corner regions. The elastic stiffness can be approximated by using the plastic design of the effective column web area:

$$K_e = \frac{V}{\gamma} = 0.95 d_c t_{cw} G$$

where t_{cw} is the column web thickness, and d_c is the column depth. This equation is valid until $\gamma = \gamma_y = F_y/\sqrt{3}G$. Therefore, the shear force at the general yielding is obtained as:

$$V_y = 0.55 F_y d_c t_{cw}$$

In the post-elastic stage, the additional shear strength, ΔV , is derived from the springs at four corners of the model, when the boundaries of the panel zone are assumed to be rigid. The rotational stiffness of the spring is approximately calculated as:

$$K_s = \frac{M}{\theta} = \frac{Eb_c t_{cf}^2}{10}$$

where θ is the concentrated spring rotation, and b_c and t_{cf} are the width and thickness of the column flange, respectively. Krawinkler et al. reported that K_s cannot be computed through the use of simple models, and has to be obtained from finite element analyses. Then, the post-elastic stiffness of the joint is given by:

$$K_p = \frac{\Delta V}{\Delta \gamma} = \frac{1.095 b_c t_{cf}^2 G}{d_b}$$

This equation is obtained from the work equation $0.95d_c\Delta V\Delta\gamma=4M\theta$, with $\theta=\Delta\gamma$ and E=2.6G. Assuming that the post-elastic stiffness, K_p , of the joint is valid for a range of $\Delta\gamma=3\gamma_y$. The ultimate strength, V_n , of joints is then given by:

$$V_{n} = K_{e} \gamma_{y} + 3K_{p} \gamma_{y} = V_{y} \left(1 + 3\frac{K_{t}}{K_{p}} \right) = 0.55F_{y} d_{c} t_{cw} \left(1 + \frac{3.45b_{c} t_{cf}^{2}}{d_{b} d_{c} t_{cw}} \right)$$

The ratio of the second term over the first term inside the parenthesis represents increase in panel zone shear strength beyond that predicted by the von Mises criterion. This model was found to capture the few available experimental results reasonably well, and has been adopted by many seismic codes, and used until now. It is important to note that this model does not include shear strain hardening in the column web panel.

In this study, the column axial load had also been included for its impact on the behavior of the panel zones. Experiments had shown that the ultimate shear strength was not significantly affected by the column axial load. The axial force was immediately transferred to column flanges when the panel zones started yielding in shear. Therefore, the proposed model was expected to give good results for both exterior and interior joints when axial column load ratio P/P_y was less than 0.5.

2.2.3.3 Krawinkler et al. (1987), Tsai et al. (1990), Schneider et al. (1998), and Deierlein (1998)

Although the concept of allowing panel zones to yield prior to/or simultaneously with the beams had been adopted since early 1980, the conventional rigid frame analysis with an assumption of rigid links between the beams and the columns was still widely used by engineers. The main objectives of these studies were to observe the effects of panel zone shear deformation on the structural strength and stiffness, and on the distributions of inelastic deformation in frame structures subjected to earthquake excitations.

Their analytical models were based on the buildings ranging in height from two to seventeen stories. Elastic response spectrum, inelastic static pushover, and elastic and inelastic time-history analyses were conducted using the ground motion data from representative earthquakes to establish loading and deformation demands. The results from different buildings were quite similar and led to the following conclusions:

- 1) Both the joint size and the panel zone flexibility were shown to significantly affect the stiffness and vibration period of the structures. The simple analytical models that did not include panel zone deformations underestimated the drift by as much as 10% and overestimated the base shear by 30%.
- 2) The simple analytical models with rigid eccentricities at the beams and the column ends, without including panel zone flexibility, should not be used in practice.
- 3) The analytical results illustrated that allowing panel zone deformations in moment-resisting frames can benefit the inelastic dynamic response of the structural systems. However, having the flexible panel zone designed by the current provisions can increase joint ductility demand from that with the rigid panel zone. In other words, it is still unclear if the current provisions of the panel zone design are adequate. The shear

strength of panel zones may need to be limited to 80% of the shear force induced by a summation of the flexural strength of the beams at the joint.

2.2.3.4 El-Tawil et al. (1999)

El-Tawil et al. evaluated panel zone strength provisions of AISC (1980), Krawinkler (1978) and FEMA 267A (1997) using finite element models of a number of exterior beam-to-column subassemblages. The panel zone strength provisions are given by Equations (2.1), (2.2), and (2.3).

$$V_n = 0.55 F_{v} t_c d_c (2.1)$$

$$V_{n} = 0.55 F_{y} t_{c} d_{c} \left(1 + \frac{3b_{cf} t_{cf}^{2}}{d_{b} d_{c} t_{c}} \right)$$
 (2.2)

$$V_{n} = \frac{0.55F_{y}t_{c}d_{c}}{0.8} \left(1 + \frac{3b_{cf}t_{cf}^{2}}{d_{b}d_{c}t_{c}} \right)$$
 (2.3)

The study concluded that Equation (2.1) reasonably predicts the strength of the panel zone at the onset of inelastic panel zone deformation for connections with various beam depths and column flange thickness. It was determined that a significant inelastic panel zone deformation must occur before the panel zone strength according to Equation (2.2) can be achieved. The equation; however, did not work well with connections having thicker column flanges. Furthermore, Equation (2.3) represented the upper bound strength of the panel zone. El-Tawil et al., suggested that the 80% factor should not be used for the design of exterior connections.

2.2.3.5 El-Tawil et al. (2005)

This paper evaluated and discussed the new panel zone design introduced by FEMA-350(2000) in its seismic design provision. The study was based on an examination of published test data and the results of transient analyses of buildings with four-, eight-, and sixteen-story moment resisting steel frames. The study concluded that according to limited test results reviewed do not confirm the adequacy of the new panel zone provisions. The analyses showed that the panel zone designed by the new provision leaded to a rather low level of panel zone participation of the three building studied. Moreover, it suggested that pane zone deformation demands could be affected by connection detailing.

CHAPTER 3

DEVELOPMENT OF FINITE ELEMENT MODEL

3.1 INTRODUCTION

The main objectives of this research are to understand the beam-to-column moment connection behavior, and to present a suitable design of the panel zone. These can be successfully achieved by using finite element analysis analyzing available test results of a full-scale beam-to-column moment connections tested during Phase II of the SAC steel project. In this chapter a FE model of specimen SP4.1 tested at the University of Michigan was developed and verified with the experimental result. Then the future analyses of the model were presented such as stress distributions in the connection area.

3.2 DESCRIPTION OF MICHIGAN SPECIMEN SP4.1

The geometry of the analysis configuration used in this study was derived from the geometry of specimen SP4.1 (Goel et. al. 1998) tested at the University of Michigan during Phase II of the SAC Steel Project. The specimen SP4.1 consisting of W30x99 beam connected to W14x176 column was made of A572 Grade 50 steel. This specimen was detail according to construction practices in which the web was connected through a bolted shear tab, while beam flanges were welded to the column flanges using field groove-welded detail as shown in Figure 2.3.

This particular specimen was selected because it was representative of post-Northridge construction practices and it showed some ductility prior to failure during the test. The specimen represents an exterior connection subassemblage from typical steel MRFs as shown in Figure 3.1. The subassemblage is made by considering that the moments at the mid-height of a story and at the mid-span of a beam are generally close to zero under typical seismic loading allowing an assumption of pin boundary conditions at those points.

Figure 3.2 shows a general drawing and photograph of the setup of Specimen SP4.1. The specimens were rotated 90 degree from their original position of the exterior connection in the building. The columns were bolted to the supports at both ends. The free end of the beam in the specimen was pin-connected to the actuator. Lateral bracing was also provided to prevent out-of-plane movement of the beam. The distance between the column flange surface and the actuator axis was kept constant at 135 inches for the tested specimens. The clear distance of the column between the supports is also constant at 144 inches.

Properties of the specimen are also presented in Table 3.1. The yield and ultimate stresses of specimens are given in Table 3.2. The material properties were obtained from tensile coupon tests of steel cut from flange and web areas.

The loading protocol was a quasi-static cyclic displacement pattern as defined by the SAC Test Protocol document (SAC1997). The displacement history can be seen in Figure 3.3 (for the University of Michigan specimens). This displacement loading was applied to the specimen until either fracture occurred, resulting in a significant loss of resistance, or a story drift of 6% radians is reached.

Table 3.1. Properties of analysis specimen SP4.1.

Name	Beam or Column Depth (in)	Web Thickness (in)	Flange Thickness (in)	Flange Width (in)
Beam	30	0.5	0.67	10
Column	15	0.68	1.09	16

Table 3.2. Coupon yield/ultimate stress data of specimen SP4.1.

Specimen	Beam (Yield/Ultimate): (ksi)	Column (Yield/Ultimate): (ksi)		
	W30x99	W14x145		
4.1 (Fl.)	51.2/69.8	47.7/69.0		
4.1 (W.)	55.1/71.6	48.3/67.7		

Note: Fl.=Flange, W.=Web

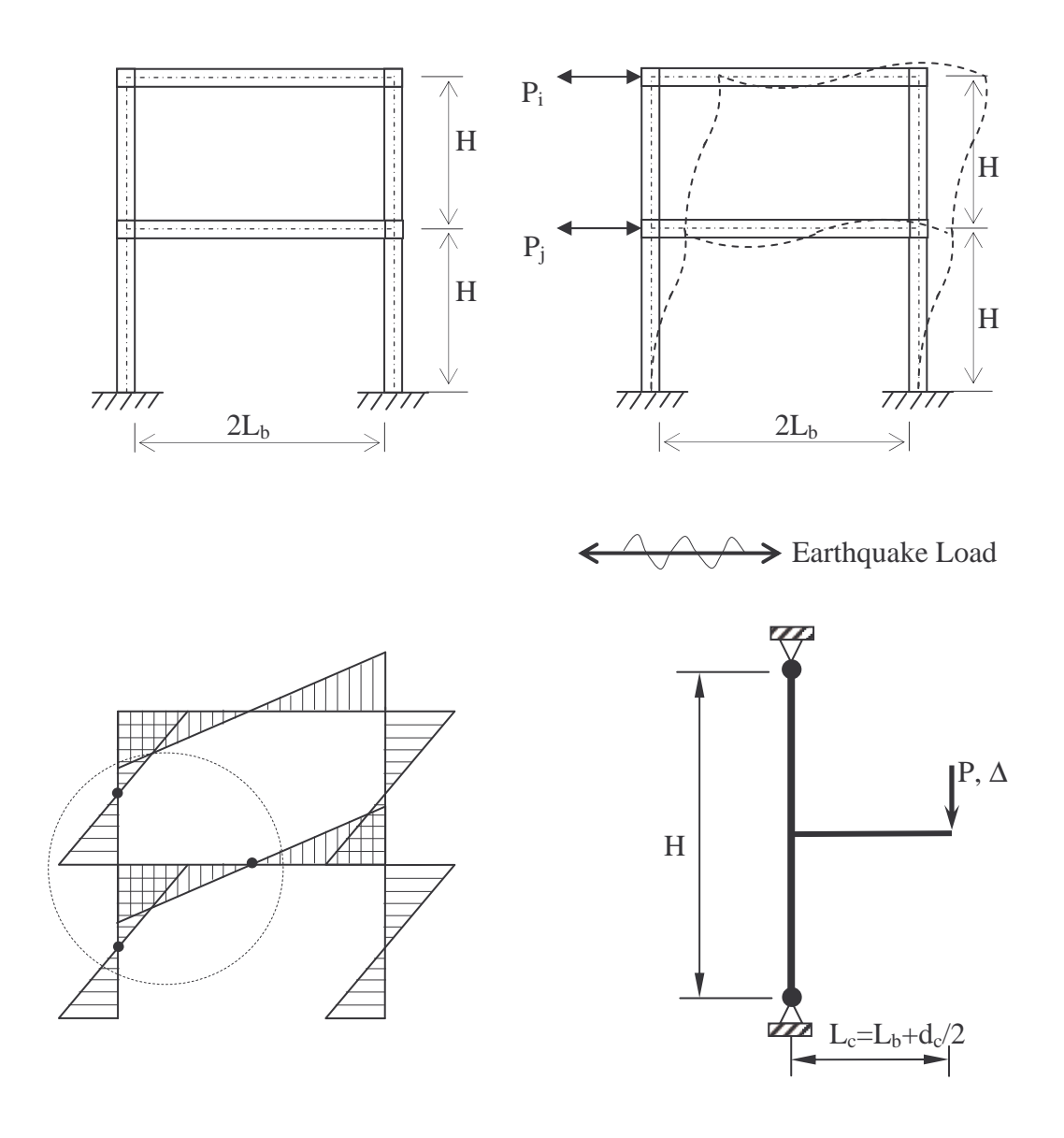


Figure 3.1. Location of the exterior connection sub-assembly in a typical steel moment frame.

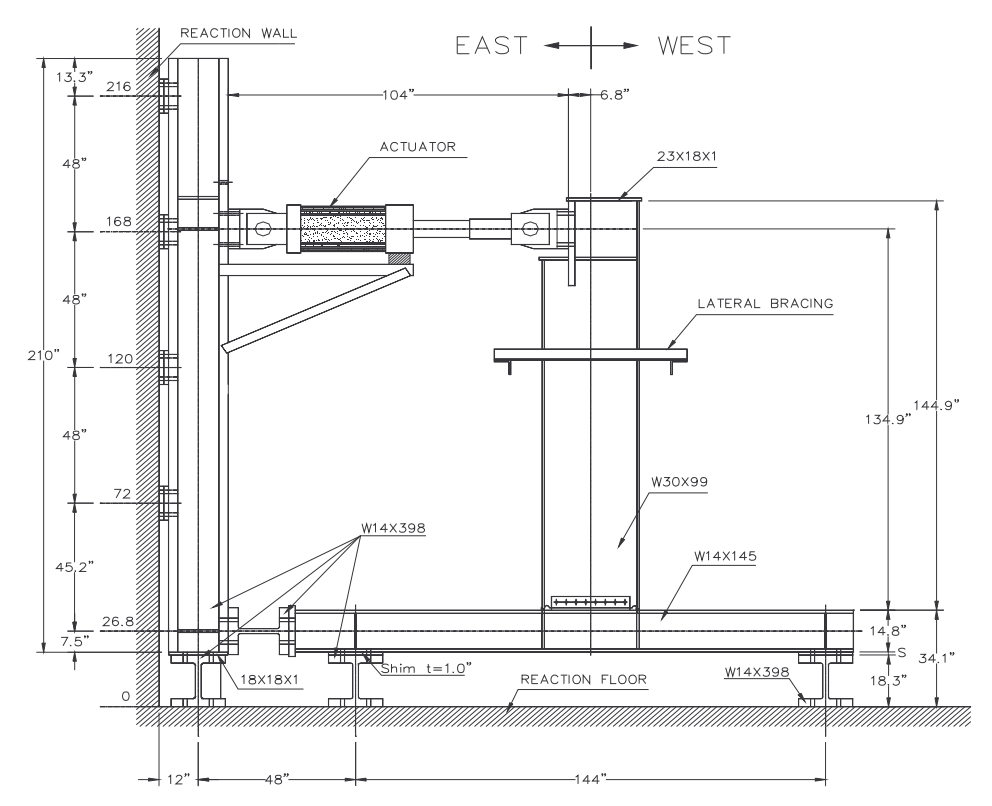


Figure 3.2. a) Drawing of the test set-up at the University of Michigan [42].



Figure 3.2. b) Photograph of the test set-up at the University of Michigan [42].

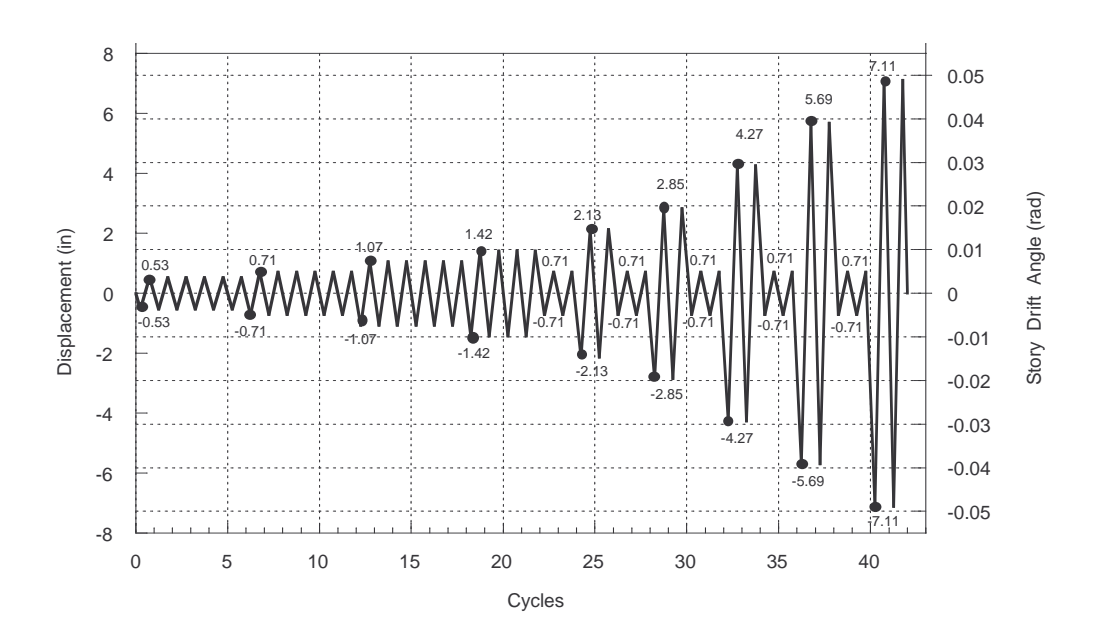


Figure 3.3. Loading history for the University of Michigan specimens [42].

3.3 FINITE ELEMENT MODEL OF SPECIMEN SP4.1

The general-purpose finite element analysis program ABAQUS (5.6 and 5.7) was used to develop a 3-D model of the moment connection. The finite element model of the connection had the member sizes similar to specimen SP4.1 tested at the University of Michigan. The span length between the center of actuator to the face of column was 135 inches, and the distance between the column supports was 144 inches as shown in Figure 3.2.

Four-node shell elements (S4R) were used to model the connection. The shell element has four nodes with six degrees of freedom at each node: translations and rotations in the nodal x, y, and z directions. Although local and through-thickness behavior can not be accurately computed using the shell element, the S4R element provides outputs of the stress distributions as layers and transverse shear stress through

the element thickness. Figure 3.4 shows the geometry and node locations for this element type.

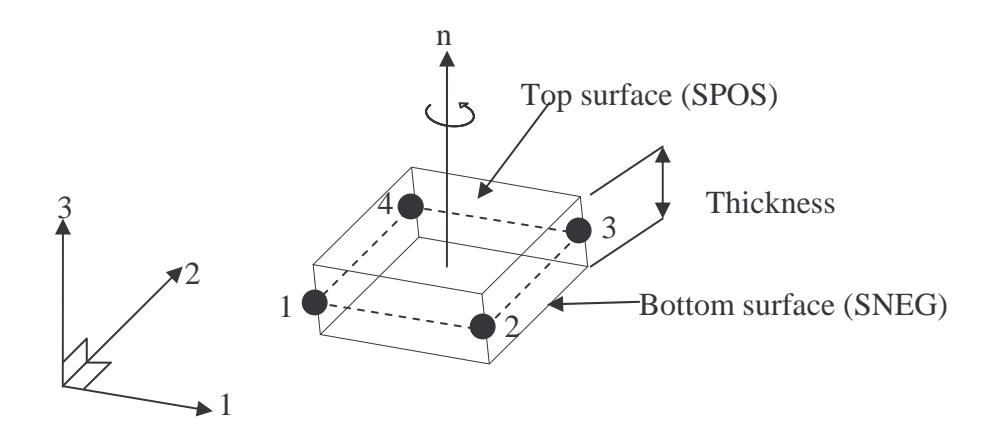


Figure 3.4. S4R: 4 node reduced integration shell element.

Figure 3.5 shows the finite element model of the specimen SP4.1. All connected interfaces between the webs and the flanges, the continuity plates and the flanges, the shear tabs and the webs, and the shear tabs to column flanges were modeled by using MPC. It should be noted that the welds, bolts, and backing bars were not modeled. The support condition at the column ends was modeled as a pin boundary condition by allowing a free rotation, but restrained the in-plane and out-of-plane displacement. The finite element models were subjected to inelastic analysis. However, only material nonlinearity of the connections was included in the inelastic analysis. The material of beams, columns, shear tab, continuity plates were assumed to be A527 Grade 50 steel. The steel has an assumed yield strength of Fy = 50 ksi. with elastic modulus of 29000 ksi. The steel was also assumed to have strain hardening modulus equal to 5% of the elastic modulus up to 1% strain. The steel was assumed to be perfectly plastic for larger strains. Figure 3.6 shows the assumed Grade 50 steel stress-strain curve used in the inelastic analysis. Differences between the base metal and weld metal properties were disregarded. The

inelastic analysis was conducted by applying cyclically increasing static displacement at the beam tip to a maximum of 7 inches (approximation of 5% story drifts) as shown in Figure 3.3.

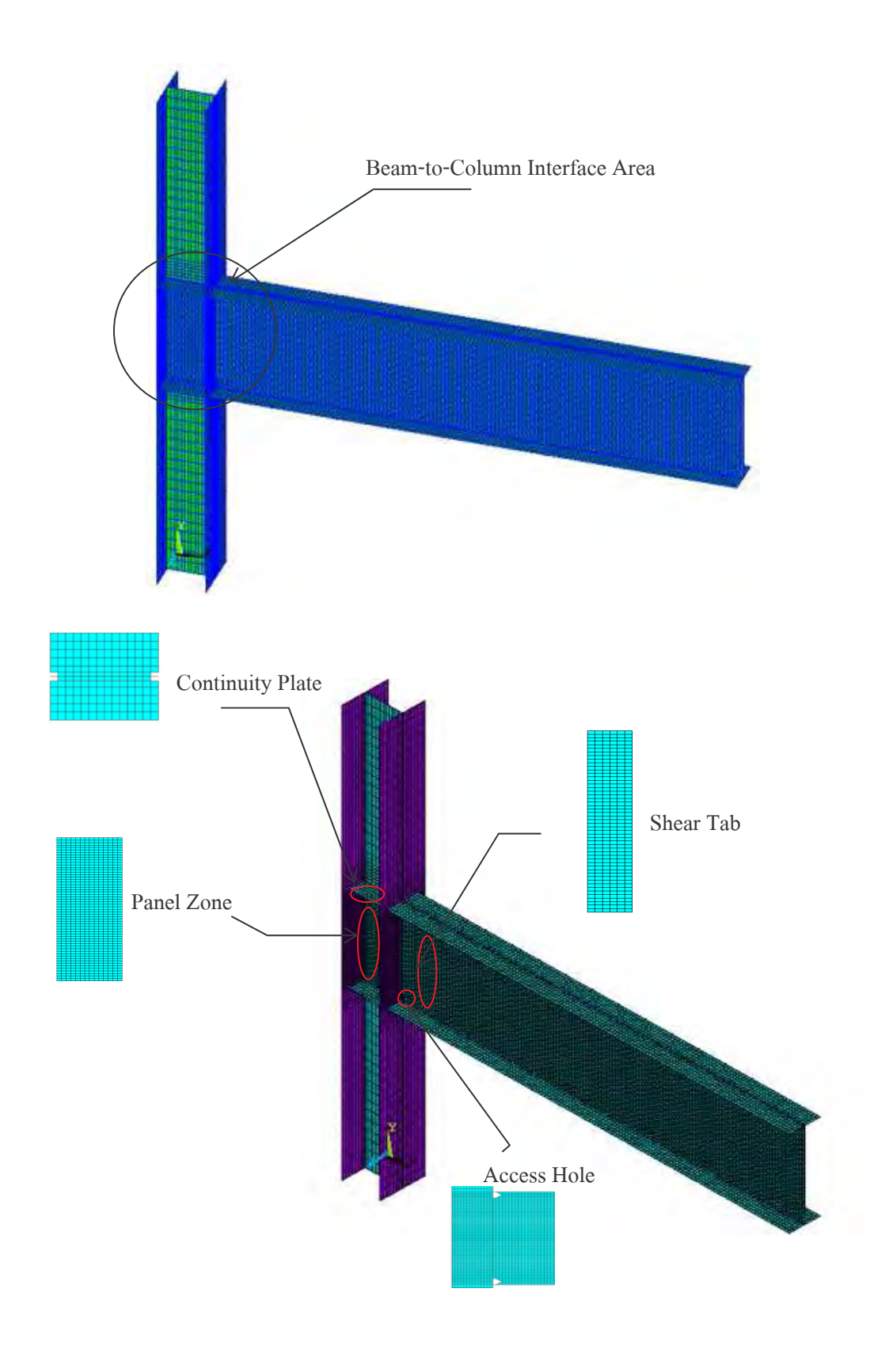


Figure 3.5. A finite element model of specimen SP4.1.

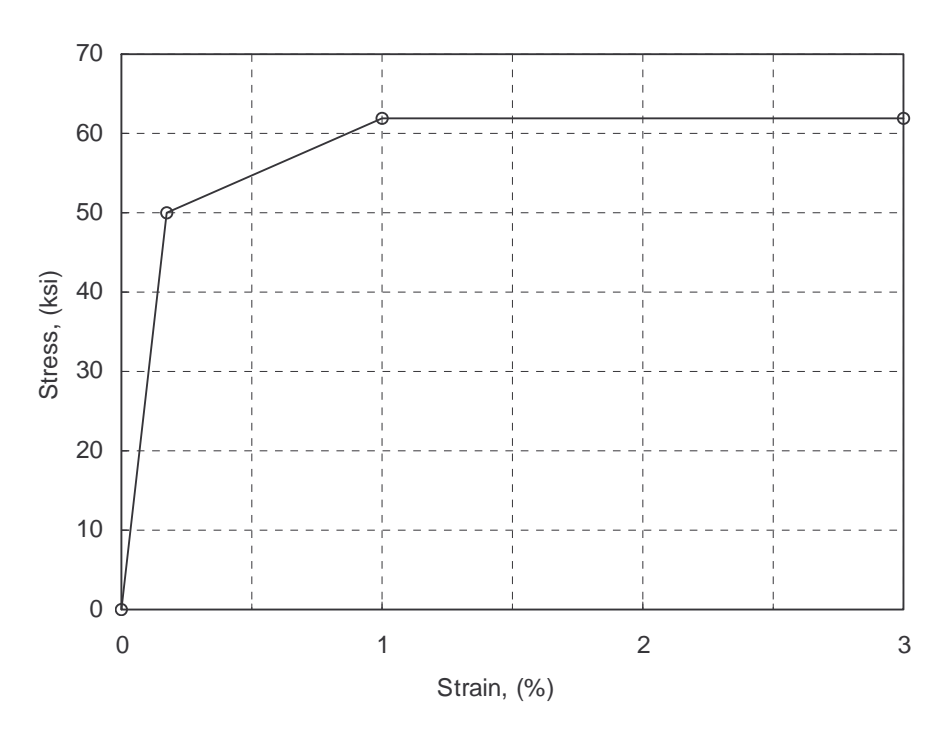


Figure 3.6. Stress-Strain curve for steel used in the inelastic analysis [42].

3.4 VERIFICATION OF FINITE ELEMENT MODEL OF SPECIMEN SP4.1

The results from FE analysis of Specimen SP4.1 as described in the previous section were compared with the experimental results. The load-displacement responses of the experiment and finite element analysis are compared in Figure 3.7. As can be seen, the analysis shows good agreement with the experiment. The initial yield load is 80 kips and 85 kips for the test and analysis, respectively. The corresponding displacement is approximately 1.4 inches and 1.5 inches, respectively. The maximum load from the test is 120 kips in positive displacement cycle, and approximately 100 kips in the reverse displacement. As can be seen, the initial stiffness and ultimate load are well represented by the FE model except the fracture of the beam flange on the negative displacement at 4.27 inches. After the fracture, the FE model can not capture the stiffness and load path of the specimen.

Figure 3.8 shows contour lines of shear and von Mises stresses in the plane of the beam and column webs at the incremental loading of 6.0 inches displacement. The yielding initiated from the center of panel zone and propagated toward the corners of the panel zone and the column flanges. The maximum shear stress in the panel zone was 36 ksi. for almost the whole area of the column web. This amount of shear stress is equal to the amount of shear force calculated from $\frac{F_y}{\sqrt{3}}$ with the value of $F_y = 60$ ksi. Therefore,

the panel zone demonstrates the complete yield of the panel zone in a pure shear condition at this level. However, shear stress decreased rapidly to almost zero directly beneath continuity plates. The direction of the shear stress in the column web changes under the continuity plates. The maximum von Mises stress was approximately 62 ksi, where the yield stress of this FE model was set at 50 ksi. During the panel zone yielding, the beam flanges started to yield within a limited area. Minimal yielding was observed near the weld access hole and in the beam web. This shows that the beam never reached its fully plastic stage. The stress contours and yield mechanisms of the panel zone and around the connection area obtained from the finite element analysis were similar to what had been observed from the test of Specimen SP4.1 as shown in Figure 3.8. The panel zone completely yielded over the entire web area, and the minimum yielding occurred in the connection area, around the weld access hole and the beam web.

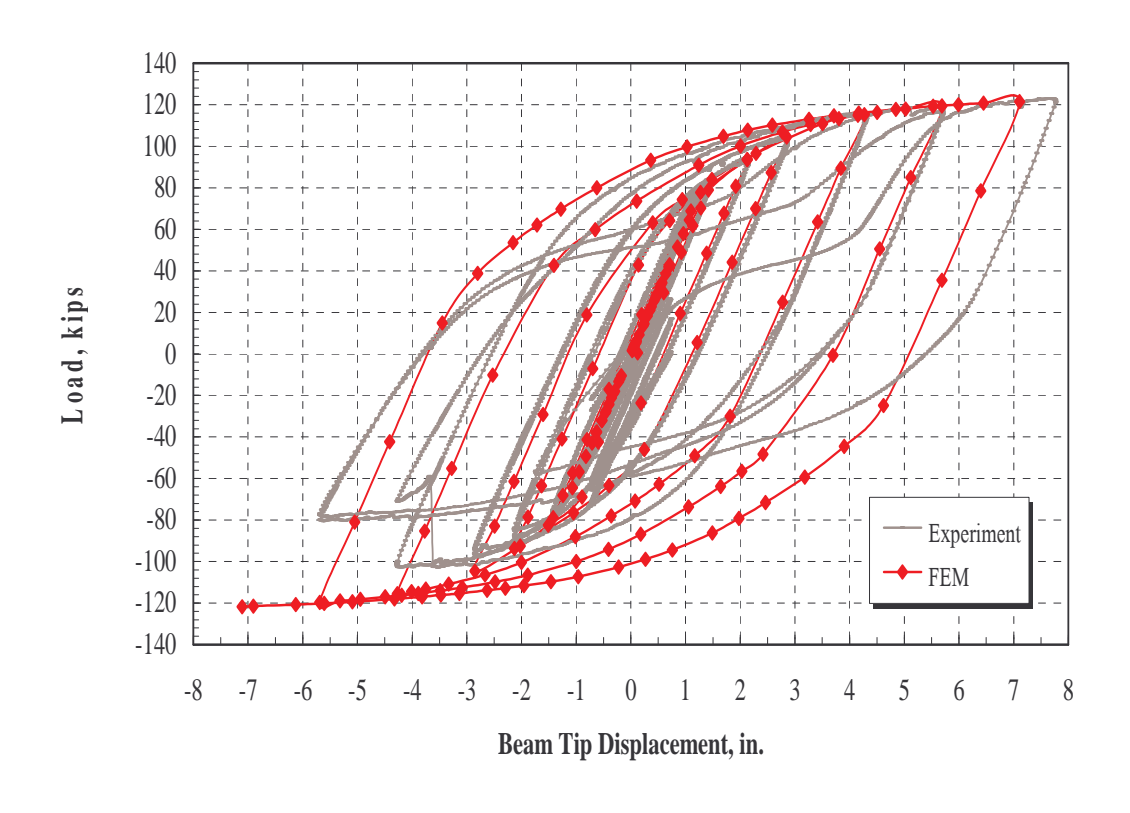


Figure 3.7. Comparison of load-displacement responses between test and FEA of SP4.1.

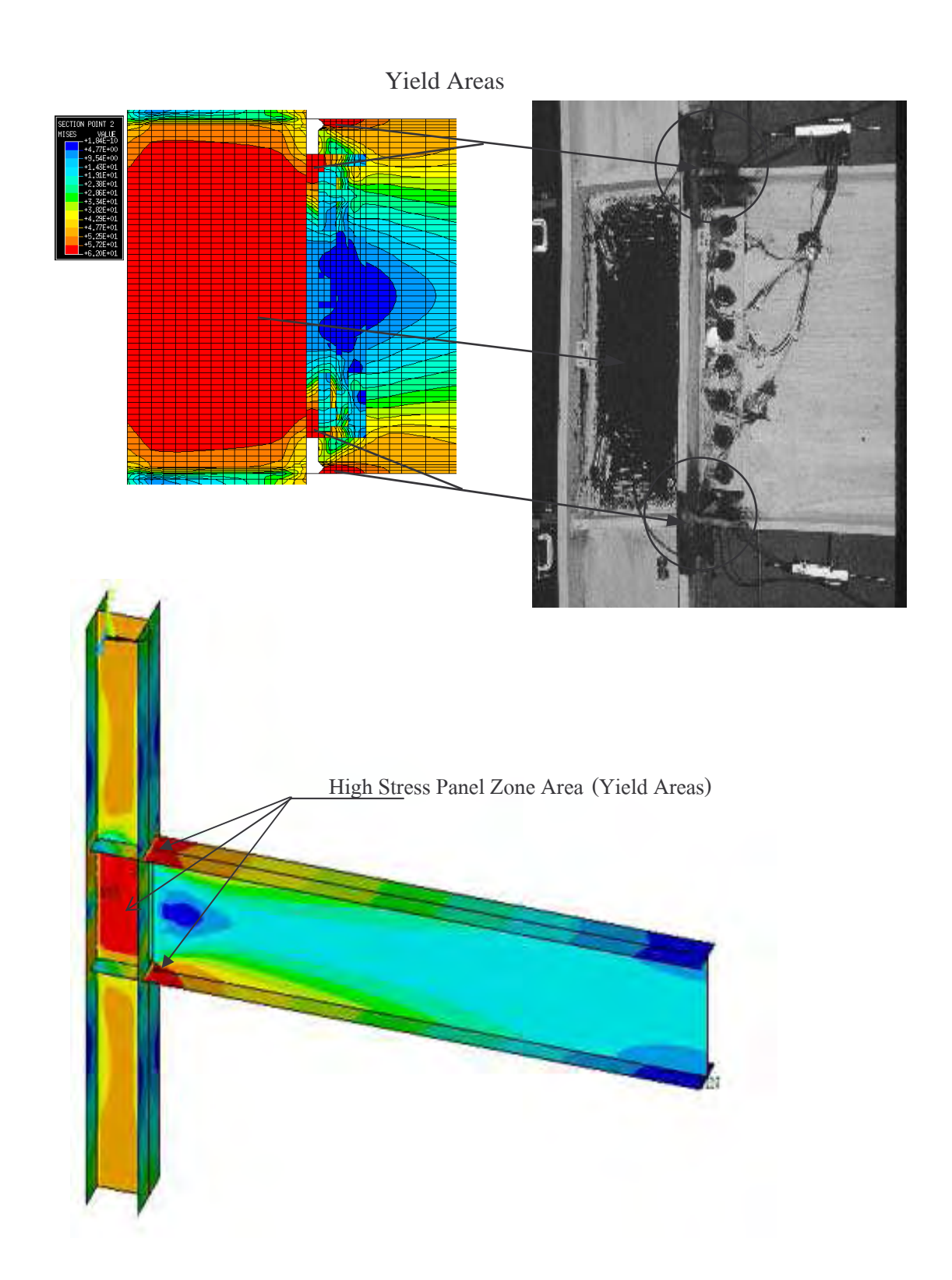


Figure 3.8. Shear stress and von Mises stress contours for Specimen SP4.1.

3.5 ELASTIC ANALYSIS OF SPECIMEN SP4.1

Since the elastic FE analysis is much easier and less time consuming to conduct, the elastic FE analysis of specimen SP4.1 is further investigated in this section. By utilizing the FE model form the previous section, beam, column, shear tab, continuity plates were assumed to have an elastic modulus of 29000 ksi. The load was applied at the tip of the beam as a monotonic increasing static force as maximum as 100 kips. The intention of elastic analysis was to study the stress distributions in the connection region, especially shear stress.

Figure 3.9 and 3.10 present the principal stress vector and von Mises stress distribution in the connection region. The vector plot shows a heavy concentration of the principal stresses flowing through the beam flange connected to the column flange. Also from Figure 3.10 and 3.11, the highest value of von Mises stress is at the center of the beam flange in a very limited region at the junction of the beam flange and the column flange. This result implies that the possibility of brittle fracture in this region is much higher than elsewhere in the connection interface area. Further investigation is made by plotting von Mises stress distributions in the beam flange at the column interface as shown in Figure 3.11. Through thickness of the beam flange was represented by three layers, top, middle, and bottom. The maximum values occur at the middle of the beam flange. The stress rapidly decreases toward the edges for all layers. In addition, the stress gradient between the top and bottom layer of the beam flange is significantly large. This gradient can cause non-uniform yielding of the beam flange. Since this non-uniform yielding occurs in a very restricted area surrounding by still elastic and stiff material, this condition can prevent the spread of yielding out further to the flange and into the beam web. Such restrained stress state may be a reason for beam flange brittle fracture instead of ductile yielding. Moreover, the stress distribution from the analysis is fundamentally

different from the results assuming from the classical beam theory which is a uniform distribution across the beam width as shown with the solid line.

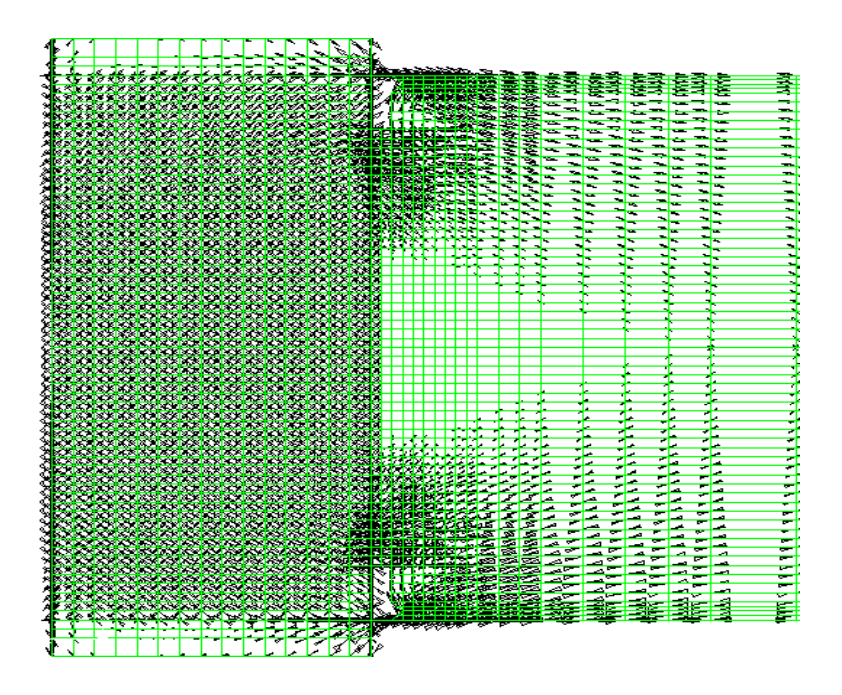


Figure 3.9. Principal stress vectors in the connection area.

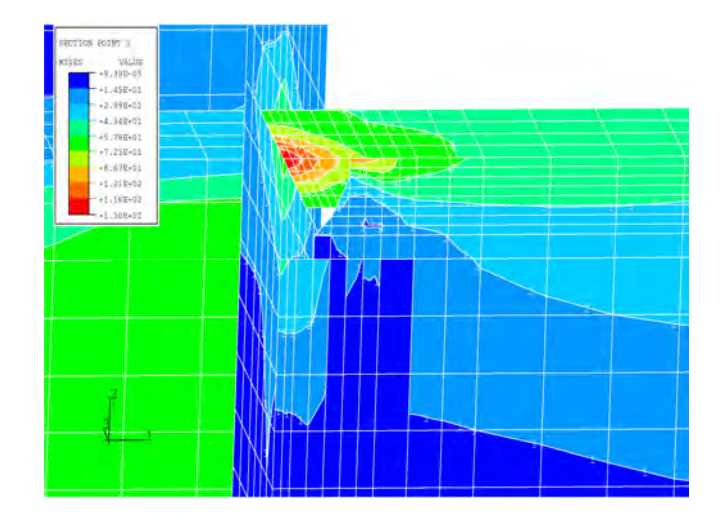
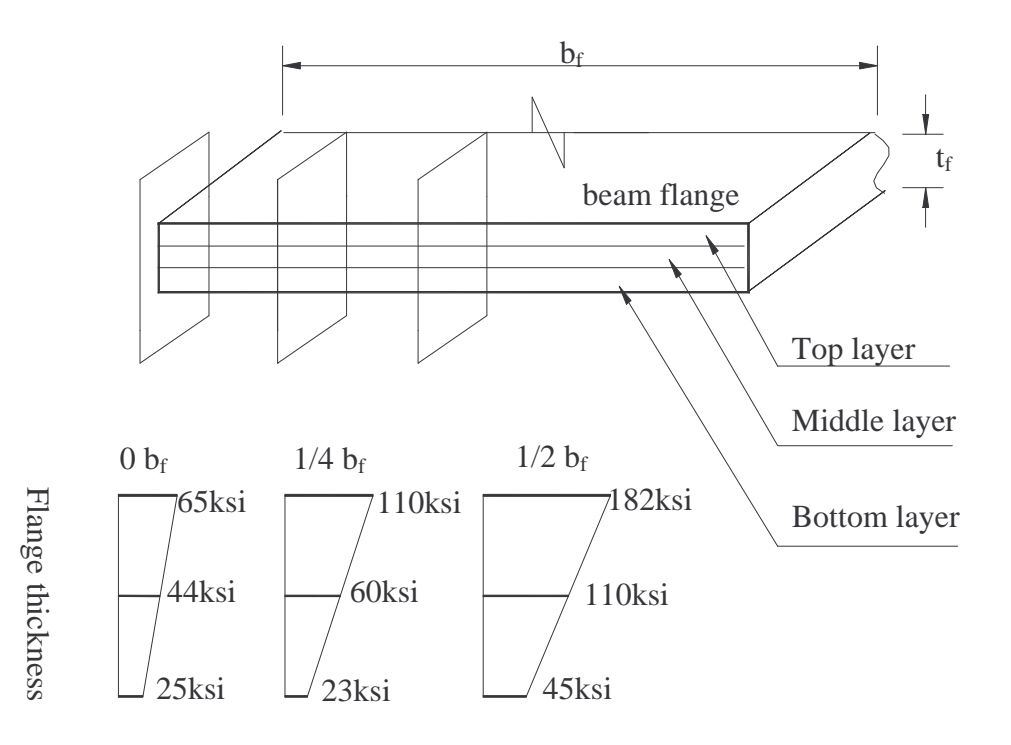


Figure 3.10. von Mises stress distributions in the connection area.



Through thickness Mises stress (bf=beam flange width)

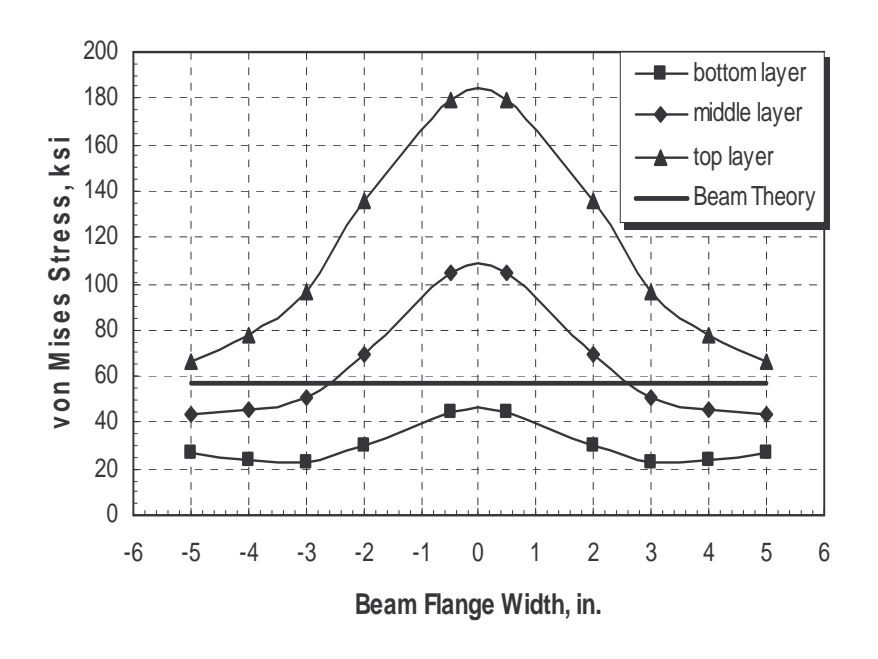


Figure 3.11. von Mises stress distributions on the beam flange.

Shear stress from the FE model was plotted in Figure 3.12 against the depth of shear tab. The y-axis represents the height of the shear tab measured from the neutral axis of the beam. The thin solid line shows the shear stress distribution computed using the FE model. The thick solid line represents the distribution obtained from the beam theory. As can be seen, the highest shear stress in the FE model did not occur at the neutral axis, as it was expected by the beam theory. In contrast, the highest stress occurred close to the corners of the shear tab. This phenomenon is caused by the boundary effect in beam-to-column connection [25].

To reinforce this result, fractions of the shear force carried by the shear tab and the beam flanges were computed by summing up the shear stress in the interface cross section. This calculation can be approximated by summing up products of the average element shear stress in each element and element cross-sectional area along the considered section. The shear force carried by the shear tab is 34 kips, computed from the plot in Figure 3.12. Since the applied force was 100 kips, the remaining of 66 kips has to be carried by the beam top and bottom flange. It can be seen that the beam flanges can be overloaded by this unexpected shear force. Figure 3.13 shows the percentages of the shear force in the top flange and shear tab, corresponding to the top half of the beam. The thickness of the beam flange was divided into two layers, top and bottom. As can be seen, the shear forces in these two flange layers have opposite directions. It is very interesting to observe that even though the summation of shear forces in the beam flange is approximately 33% of the total shear, the top half of the beam flange carries about 57%, and the bottom half carries 24% of the total shear, but in the opposite directions. This suggests that the beam flange undergoes intense local bending along the span between the weld and the access hole. This can be one possible reason for fracture of the beam flanges observed in pre-Northridge connections. The same calculation of the shear distribution is performed for the cross-section of the beam web at 30 inches away from the interface area. The shear force in the beam web is about 97 kips. Thus, the flanges carry approximately 3 kips of shear force. This shows that the beam theory is applicable at distances away from the interface area of the connections, but not at the interface area.

From Figure 3.14, the stress locally concentrates in the upper corner of the shear tab, while there is almost no shear stress in the middle portion of the shear tab. This indicates that some stresses flow through the supplemental welds at the corners of the shear tab, while there are no shear stresses in the middle of the tab. Therefore, the welding needs for the shear tab should be reviewed. It may be necessary to reinforce the welds at shear tab corners, while there may be no need for welding in the middle of the shear tab.

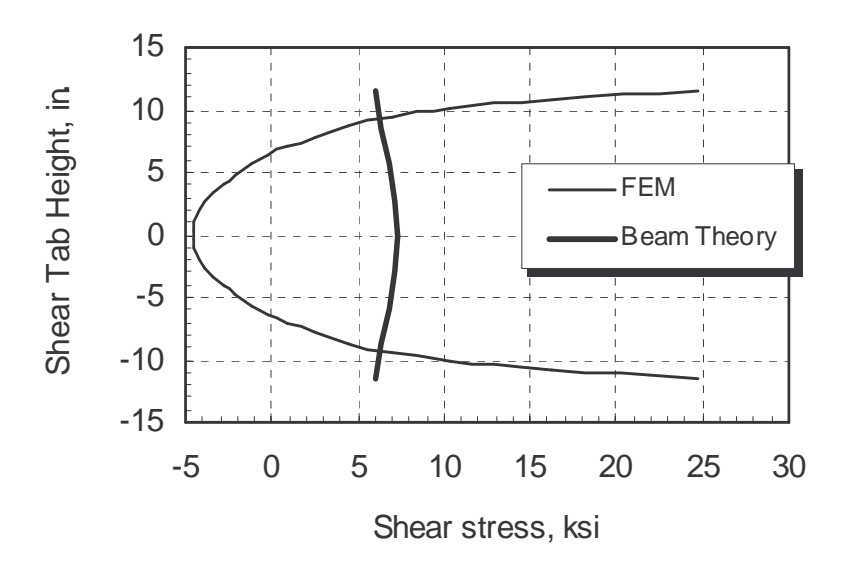


Figure 3.12. Shear stress distributions in the shear tab, 0.25 in. from the column face.

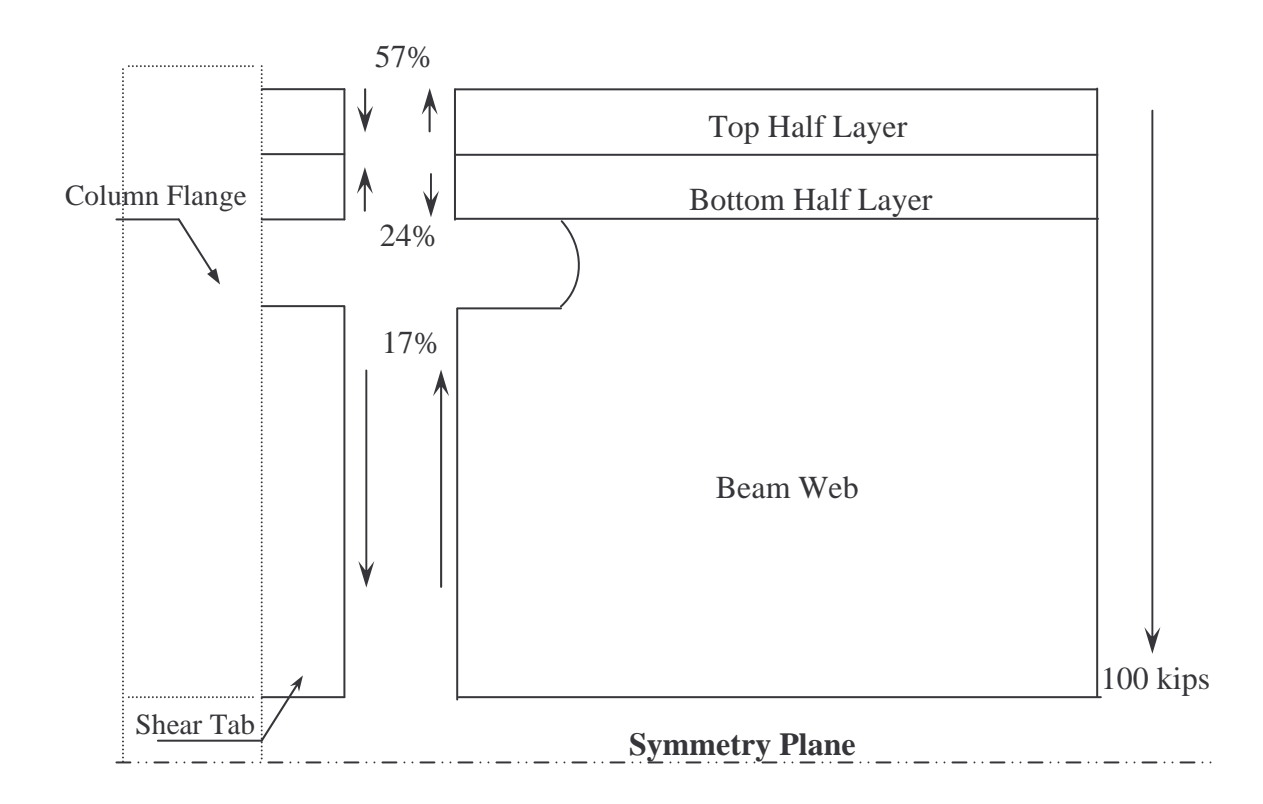


Figure 3.13. Shear force distributions in the top half and bottom half of the beam flange.

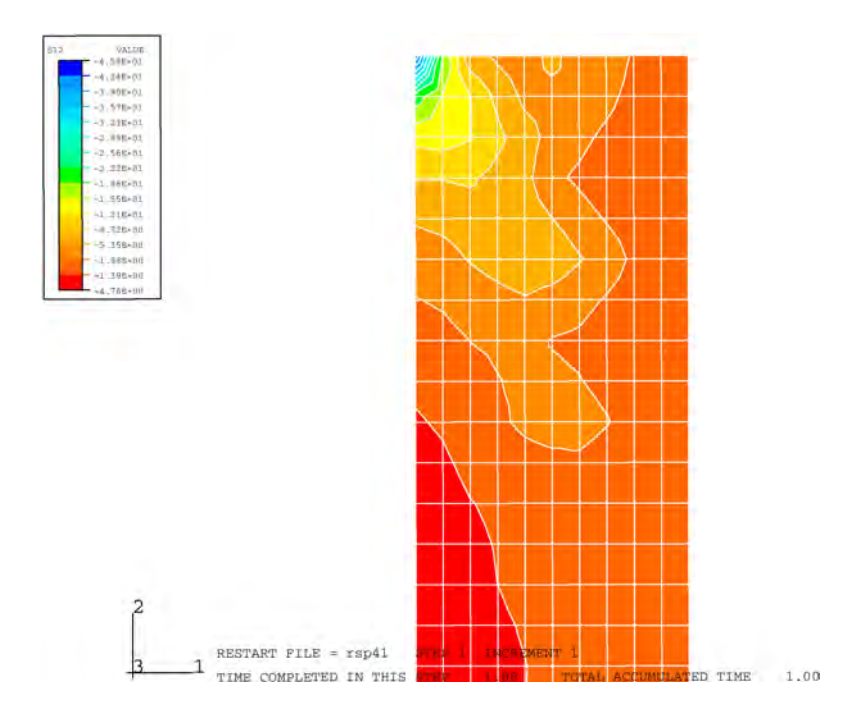


Figure 3.14. Shear stress (S12) contours in the shear tab.

3.5.1 Conclusions from Finite Element Analysis of Specimen SP4.1

The FE analyses showed that the stress distributions near the connection are much more complex than what are usually assumed in designs. The tensile stress is critical at the center of the beam flange, and at the weld to the column flange. The results also showed that the beam flanges are not only subjected to a high tensile stress, but it is also subjected to considerable shear stress over thickness of the flanges. The multi-axial stress and relatively high stress intensities can be one of the reasons causing early flange fractures in the pre-Northridge connections. The most vulnerable region is the area between the column face and the beginning of the weld access hole. This finding was confirmed by the experimental results at the University of Michigan and at other universities. The comparisons between the test and finite element analyses (elastic and inelastic) indicated that the finite element models developed in this part of the study, which include types of elements, model assumptions, cyclic and monotonic loading, strain hardening etc., are quite accurate and can be used to perform the connection parametric study. The current finite element is capable of providing reasonable results for both local as well as global behavior of the connection.

Table 3.3. Summary of maximum stress and shear force distributions in the beam flange.

Stresses or Forces	Distance from the Column Face			
	0.25 in.	0.5 in.	1.25 in.	
S11 (ksi)	175	127	108	
S22 (ksi)	55	-10	3	
S33 (ksi)	25	-12	-37	
Von Mises (ksi)	163	138	90	
% Shear Force per one Beam Flange	33 %	32%	32%	

CHAPTER 4

STUDY OF PANEL ZONES

4.1 PANEL ZONES OF AN EXTERIOR COLUMN

The stiffness of a typical steel moment connection is derived from three basic components: beam, column, and panel zone. A panel zone is a rectangular portion of a column web contained within the joint region and continuity plates. Figure 4.1 shows the free body, shear force, and bending moment diagrams in the typical exterior column under lateral loads. As can be seen, the panel zone is subjected to a high shear force created by the unbalanced moment at the column face. The effects of the shear force are very important and must be accounted for in the design of frames. In the design for strength, the connections must be capable of transmitting this shear force through the columns in accordance with the selected design procedure. In the design for stiffness, it is necessary to verify that the connection distortions caused by the shear force do not excessively affect the story drift under the lateral loads. Unfortunately, failure modes in the connection area observed after the Northridge earthquake suggested that the panel zone design code is inaccurate. The panel zones did not perform as was expected by the design philosophy. After the earthquake, researchers are still debating on the design procedure of the panel zones. Some current studies showed that the use of weak panel zone design may increase possibility of brittle fracture of the beam flanges. In other words, allowing the inelastic action in the panel zone may not be beneficial as thought earlier. These clearly indicate that the study of the panel zones in terms of strength,

stiffness, and ductility is required, before any rational design procedures of the panel zones can be formulated.

Shear force demand (design shear force), V_u , from the beam in the exterior beam-to-column connection can be derived from the moment couple of tension and compression forces at the center of column. Resolving equilibrium on the free-body diagram of panel zone as shown in Figure 4.1, and taking the forces acting on the face of panel zone as positive, the horizontal shear demand for the panel zone at the center of column can be calculated as follows:

$$V_u = \frac{M_{pz}}{0.95d_b} - V_c$$

$$M_{pz} = V_b L_c$$

$$V_b = \frac{M_b}{L_b}$$

$$V_c = \frac{L_c}{H} V_b$$

Thus,

$$V_{u} = \frac{M_{pz}}{0.95d_{b}} - \frac{M_{pz}}{H}$$

$$V_u = \frac{V_b L_c}{0.95 d_b} - \frac{V_b L_c}{H}$$

$$V_{u} = \frac{V_{b}L_{c}}{L_{b}} \left(\frac{1}{0.95d_{b}} - \frac{1}{H} \right) \tag{4.1}$$

where M_{pz} is the moment at the center of column, V_b is the beam tip load calculated from assuming the unbalanced beam moment, M_b , was developed at the face of column, L_b is distance from the beam tip to the face of column, L_c is distance from the beam tip to the center of column, H is the column height of the subassemblage, V_c is the column reaction force, and $0.95d_b$ is approximation for the effective beam depth. The beam moment, M_b , given by AISC Seismic Provision 2005 is equal $C_{pr}R_yZ_bF_y$, and $C_{pr}=\frac{F_y+F_u}{2F_v}\leq 1.2$.

It should be noted that the above equations are given for the general exterior connection. Magnitude of the beam moment, M_b , depends on the panel zone design approaches, which will affect yielding of the panel zone. In addition, M_b is assumed to be at the face of column, which may not be the actual location of the maximum beam moment for some special connection types such as flange plate-and-vertical rib connections, reduced beam section connections, Free-Flange connections etc.

Based on AISC Seismic Provision 2005, design shear strength of the panel zone, $\phi_v V_{n,}$ is given by Equation (4.2):

$$\phi_{v}V_{n} = \phi_{v} 0.6F_{y}d_{c}t_{p} \left[1 + \frac{3b_{cf}t_{cf}^{2}}{d_{b}d_{c}t_{p}} \right]$$
(4.2)

with the condition of P_u less than 0.75 P_y . P_u is the required axial strength in compression of column. P_y is the yield strength of column. In addition, t_p is the total thickness of panel zone including doubler plates, d_c is the overall column section depth, b_{cf} is the width of column flange, t_{cf} is the thickness of column flange, d_b is the overall beam depth, F_y is the specified minimum yield strength of panel zone steel, and ϕ_v is the resistance factor for shear which is taken equal 1.0

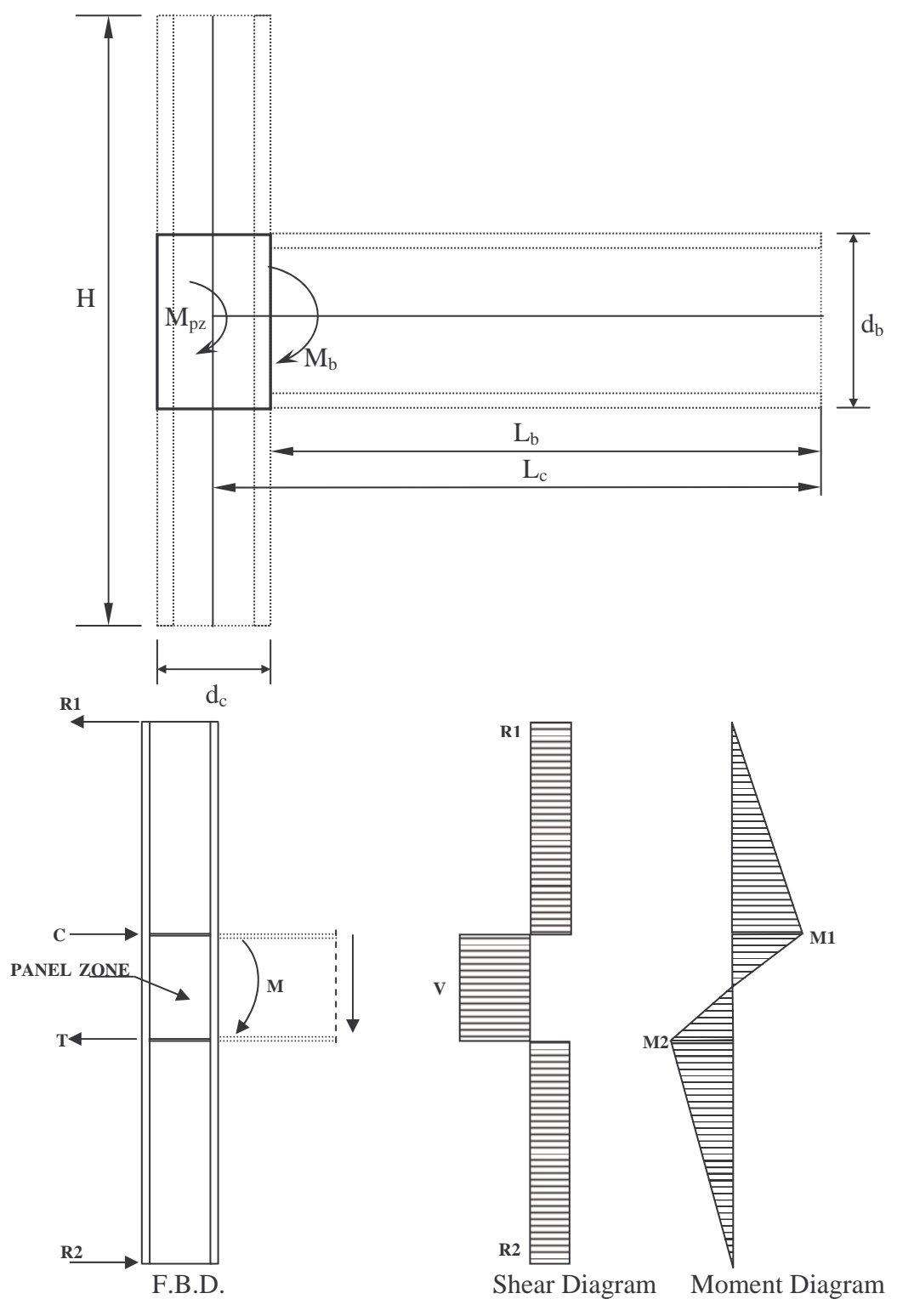


Figure 4.1. Parameters, free-body, shear, and moment diagrams of a typical column in exterior connection specimens.

4.2 PANEL ZONE DESIGN APPROACHES

Prior to 1988, the strong panel zone philosophy was used by most design codes in the United States. Using strong panel zone means that all column parts have to be able to remain in the elastic range and all inelastic rotations of connections must be delivered from the beam. However, inelastic rotations from beam alone were proved to be uneconomical and the connections cannot survive during a major earthquake. Even with new connection types as developed after the Northridge earthquake, such as Free-Flange, and reduced beam section etc., the beams alone tend to have difficulty in providing the minimum plastic rotations as required by the design codes without losing significant stiffness, which directly leads to rapid degradation of overall stiffness of the frames. Thus, the current design codes have allowed some yielding in the panel zone simultaneously with yielding in the beam so that the total plastic rotations can be added from the beam and panel zone.

After 1988, all panel zone design requirements in the United States were changed to the weak panel zone approach, mainly based on the studies of Krawinkler et al. and Popov et al.. Krawinkler et al.(1971-1978) which had indicated that the panel zones with careful details could exhibit excellent energy dissipation under large inelastic deformation without any stiffness degradation. The panel zones in their experiments showed considerable reserved strength beyond the first sign of yielding. This reserved strength is attributed to elements surrounding the panel zones, together with strain hardening of the column web in shear. Thus, Krawinkler suggested a panel zone design equation that can predict the ultimate shear strength of the panel zones in the inelastic stage. Later on, Popov et al. (1989) developed a different design approach of weak panel zones.

Nevertheless, Krawinkler (1978) and Popov (1989) observed that large panel zone deformation can lead to local kinks in the column flanges, which may cause additional

stress concentrations in the welded areas between the column face and the beam flanges. This, in turn, may contribute to premature fracture of the beam flanges. Statistical analyses by Roeder (1995) of many cyclic tests conducted on fully restrained steel connections also confirmed this finding. In addition, fracture analyses by Chi et. al. (1997) showed that panel zone yielding may cause a moderate increase in toughness demand on the welds. FE analysis results of beam-to-column connections performed by Tawil (1998) also yielded results with the same trend. Moreover it has been found in recent years that the actual yield strength of A36 steel is far in excess of the nominal value. Thus, an A36 beam is much stronger than the assumed value in designs. This results in much larger shear forces acting in the panel zone than expected. Overloading the panel zone in this manner can result in larger inelastic deformations than intended from the design specifications, and magnifies the problem mentioned above. It is important to note that all of the above researchers failed quantify appropriate or excessive yielding of the panel zone.

Although the panel zone itself can undergo large inelastic deformation and dissipate significant seismic energy without considerable strength degradation, a weak panel zone may have substantial detrimental effects on the connections. This reduces confidence of using the weak panel zone design as suggested by the current design codes. Thus, more works need to be done to have better understanding of the panel zone behavior.

4.3 SHEAR STRENGTH AND SHEAR DEMAND OF PANEL ZONES

The current formula used for predicting the ultimate shear strength capacity of the panel zone (AISC Seismic Provision 2005) was initially suggested by Krawinkler in 1978. This formula contains sum of two stiffness parts; elastic part contributed by the column web panel, and inelastic part contributed by peripheral elements of the panel zone such as the column flanges. The elastic stiffness was derived from von Mises yield criterion of the column web panel under a pure shear condition. The inelastic stiffness was developed from the bending stiffness of column flanges. More details can be obtained from reference [22]. The panel zone rotation expected from this equation should not exceed $4\gamma_v$ (4 times of yield panel zone rotation).

The strong or weak panel zone design can be determined from the relative amount of the shear capacity and shear demand of the panel zone. If the shear capacity of the panel zone is less than the shear demand from the beams, the panel zone is weak. On the other hand, the strong panel zone can be explained in the reverse manner.

To achieve the strong or weak panel zone design concept, there are three different approaches for designing the panel zone. First, by controlling the shear capacity of the panel zone regardless of the shear demand from the beams. This approach is followed by specifying the ranges of pane zone responses. For example, strong panel zone design can be accomplished by keeping the panel zone shear strength in the elastic range. On the other hand, the magnitude of the panel zone shear strength can be assigned in the inelastic range for the weak panel zone design. The second approach controls the magnitude of the shear demand from the beams regardless of shear strength of the panel zone. As shown in Equation (4.1), the shear demand on the panel zone, V_u , depends only on the beam moment. In other words, the magnitude of the unbalanced moment can limit yielding in the panel zone. Popov and Tsai (1989) reported that strong panel zone behavior can be observed with the unbalanced moment equal to ΣM_D . The weak panel zone can be seen

with the unbalanced moment equal to $\Sigma 0.8 M_p$ or smaller. However, the panel zones designed by first or second approach alone are proved to be uneconomical. So, third approach is the combination of the first and second approaches. Despite a lack of intensive studies, the third approach was adopted by many modern design codes and guidelines in the United States after 1988. In this approach, the panel zone is allowed to yield to some degree relative to the yielding in the beams. Nevertheless, only a few studies have investigated the consequences of these relative levels of inelastic actions in the beams and panel zone, in light of the damages observed from the connections after the Northridge earthquake. Thus, it is reasonable to conclude that the modern design (third approach) of the panel zone is still questionable.

4.4 ANALYTICAL STUDY OF WEAK AND STRONG PANEL ZONES

4.4.1 Methodology and Finite Element Models

An attempt was made to study the behavior of panel zones such as yielding, deformation, stress distributions, and effects of relative strength of beams and panel zones. Finite element (FE) analysis was utilized as the primary analysis tool. All FE models used in this part were modeled using shell elements (S4R) and executed with the nonlinear analysis (small displacement-large strain) using displacement control scheme. All assumptions of the nonlinear FE analysis and models specified in Chapter 3 such as strain hardening, applied displacement etc., were applied herein as well. The global dimensions and boundary conditions of FE models were the same as those of the previous chapter.

According to the current panel zone design equation, there are 7 parameters, which have effect on the shear strength of the panel zone. Those parameters are F_y , $t_{cw}(t_{\scriptscriptstyle D})$, d_c , b_{cf} , t_{cf} , L_c , and d_b . To investigate the effects of these parameters on the

connection responses, a series of 16 FE models was developed using SP4.1 as the primary model. The geometric details for these models are shown in Table 4.1. A W30x99 section was used as beams for all models. The yield strength of the beams was 50 ksi, except in BC1, which had the yield strength of 70 ksi. This marks an upper limit for the yield strength of commercially available A36 steel (Frank 1997).

The other main intent behind changing panel zone parameters and using the same beam section is to investigate the effects of the relative shear capacity and shear demand of panel zones. Table 4.2 shows the shear strength ratios of the created models. The shear capacity, $\phi_v V_n$, was computed using the panel zone design Equation (4.2). On the other hand the maximum shear demand, V_u, was calculated using Equation (4.1) with the assumptions of the maximum beam moment, M_b, equivalent to the beam plastic moment: $M_p = Z_x F_y$. The value of beam moment, M_b , given by AISC Seismic Provision 2005 didn't implement for this study. All plastic hinges were expected at the column faces. L_b and H were taken as 134-136 and 144 inches, respectively. All specimens were designed using the strong column-weak beam criteria, but having different degrees of panel zone strengths as shown. BC1, BC2, BC3, BC4, and BC5 were designed to have weak panel zones. The panel zone of BC1, an example of a weak panel zone, has strength of only 49% of the input shear force from the beam when the beam section reaches its expected plastic moment capacity. The panel zones of BC6 to BC16 were categorized as the strong panel zone. Thus, excessive yielding in the panel zones should be expected from BC1, BC2, BC3, and BC4. On the other hand, BC6 to BC16 should have considerable yielding in the beams and no yielding in the panel zones. For BC5, BC6, BC7, and BC8, the strength of panel zone can be considered as a medium. The yielding of these specimens can be expected in a balanced manner between the beams and the panel zones. The purposes of the analyses are aimed to answer the following questions:

1) What is the influence of weak and strong panel zone design on the connection performance?

- 2) What is the influence of panel zone yielding on stress distributions in the interface area?
 - 3) What is the appropriate degree of panel zone yielding?

To permit direct comparisons between different models, the analytical results were calculated and presented at the same magnitudes of the beam tip displacement up to 4% story drifts (6.0 inches). Since the rotation responses of the panel zones for each specimen are different at the same story drifts, therefore, it is unpractical to compare the influence of the panel zone yielding between weak and strong panel zones at the same panel zone rotation.

Table 4.1. Properties of analyzed models.

Name	Fy (ksi)	d (in.)	t _w (in.)	b _f (in.)	t _f (in.)
All-Beam	50	29.65	0.5	10.5	0.67
BC1-Beam	70	29.65	0.5	10.5	0.67
BC1-Column	45	14.75	0.68	15.5	1.09
BC2-Column	50	14.48	0.59	14.67	0.94
BC3-Column	50	15	0.56	16	1.09
BC4*-Column	50	14.75	0.68	15.5	1.09
BC5-Column	50	15.25	0.83	15.65	1.31
BC6-Column	50	15	0.92	16	1.31
BC7-Column	50	15.48	0.89	15.71	1.44
BC8-Column	50	15	1.05	16	1.31
BC9-Column	50	15.72	0.98	15.8	1.56
BC10-Column	50	15	1.19	16	1.31
BC11-Column	50	16.04	1.07	15.89	1.72
BC12-Column	50	16.38	1.175	16	1.89
BC13-Column	50	15.25	1.5	15.65	1.31
BC14-Column	50	16.38	1.42	15.71	1.44
BC15-Column	50	16.74	1.29	16.11	2.07
BC16-Column	50	16.38	1.5	16	1.89

BC4* has the same beam and column sizes and also the same dimensions set up as specimen SP4.1 tested at the University of Michigan.

where d is the beam or column depth. t_{cw} is the column web thickness. b_f is the column flange width. t_f is the column flange thickness. L_c is the distance measured from the beam tip to the center of the columns ($L_b+d_c/2$).

Table 4.2. Ratios of shear strengths to shear demand of panel zones.

Name	t _{cw} (in.)	L _c (in.)	$\phi_v V_n (kip)$	V _u (kip)	$\phi_v V_n / \ V_u$
		$(L_b+d_c/2)$			
BC1	0.68	141.38	321	658	0.49
BC2	0.59	143.5	295	463	0.64
BC3	0.56	143.5	309	463	0.67
BC4	0.68	141.38	357	470	0.76
BC5	0.83	141.63	461	471	0.98
BC6	0.92	143.5	496	463	1.07
BC7	0.89	143.74	511	464	1.1
BC8	1.05	143.5	555	463	1.2
BC9	0.98	143.86	578	464	1.24
BC10	1.19	143.5	618	463	1.33
BC11	1.07	144.02	656	465	1.41
BC12	1.175	142.19	751	473	1.59
BC13	1.5	141.63	768	471	1.63
BC14	1.42	144.19	796	465	1.71
BC15	1.29	144.37	855	466	1.83
BC16	1.5	142.19	911	473	1.93

4.4.2 Behavior of Strong and Weak Panel Zone

The analysis results of two specimens, BC1 and BC16, were selected to present the effects of the weak and strong panel zone on the connection performance. Figure 4.2 shows a comparison of deformed shapes near the connection regions at 4% story drifts. The images are magnified by the same magnification factor. As mentioned earlier, a panel zone strength of BC1 is only 49% of shear demand on it, while BC16 has a panel

zone strength 93% higher than its demand. The figure shows that the deformations of BC1 are dominated by the panel zone. The panel zone distorts only in- plane direction. No out-of-plane deformation is observed in the panel zone. The other noticeable feature is that this excessive distortion of the panel zone induces a high degree of bending in the column flanges and continuity plates. It should be noted that no kink is observed at the column flange. On the other hand, deformation in BC16 is mainly provided by elongation of the beam flanges and corners of the shear tab. A severe transverse shrinkage and ponding of the beam flange in the area of access hole is also observed in the model with the stronger panel zone. This investigation confirms the results observed from other previous experiments that when panel zones do not yield, the beam flanges are subjected to heavy damages. Figure 4.3 shows von Mises stress distributions in the panel zones of those two specimens. The images are also at the 4% story drifts. The maximum stresses occurred initially at the center of panel zones and gradually propagated toward the corners of the panel zones and the column flanges, similarly in both specimens. For BC1 (weak panel zone), the panel zone completely yielded. The maximum von Mises stress is approximately 60 ksi, where the yield stress of FE model is defined as 45 ksi. Thus, the panel zone is in the strain hardening stage. For BC16, the maximum von Mises stress in the panel zone is 43 ksi, which is 7 ksi lower than specified yield stress. It suggests that the strong panel zone is still in the elastic stage, therefore, no yielding is observed.

In general, if the minimum plastic rotation of 3% as specified in AISC [3] needs to be achieved, in case of the strong panel zone, plastic rotation has to accommodate considerable deformation of the beam flanges and shear tab. However, looking at the deformation shapes and von Mises stress distributions in this region, the yielding is confined in a small area and propagates very slowly. Therefore, such the high stress concentration should be expected in the beam flange region at this level of plastic rotation.

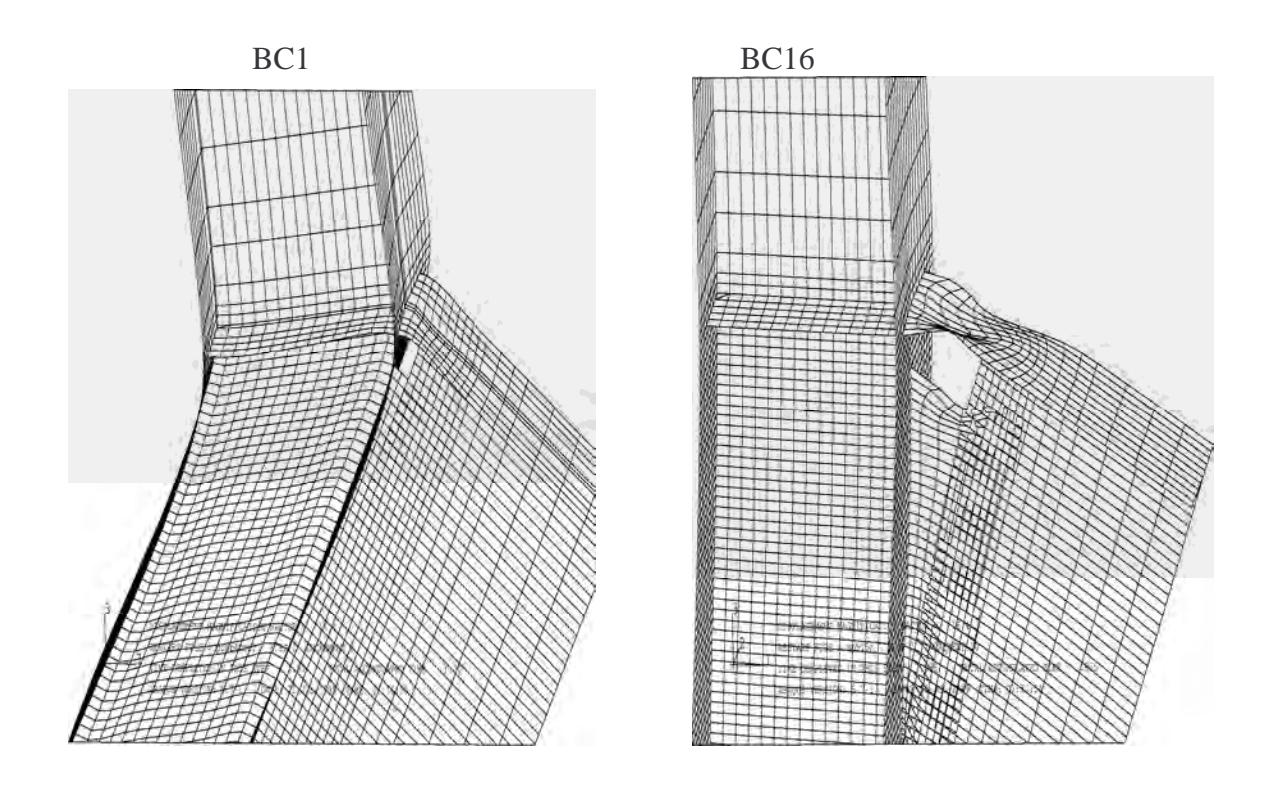


Figure 4.2. Deformed shapes of model BC1 and BC16.

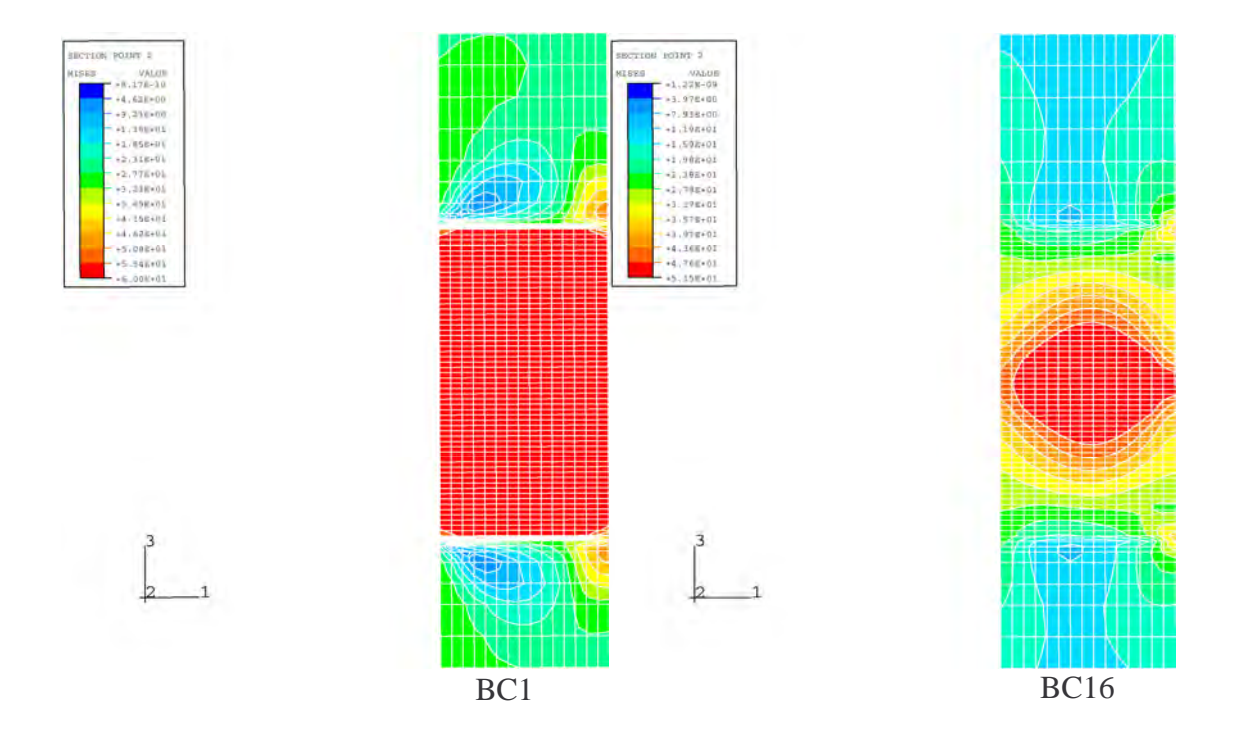


Figure 4.3. von Mises stress contours in panel zones of model BC1 and BC16.

4.4.3 Influences of Panel Zone Yielding to the Connection Interface Area

Lee et. al. (1997) have shown that the shear stress distribution at the connection area does not follow the shear stress distribution predicted by the beam theory. The additional shear stress is redistributed from the shear tab into the beam flanges. This additional shear stress can impose as a shear force carried by the beam flanges. The amount of this overlooked shear force can be significant and will overload the beam flanges, which can lead to premature failures such as fracture of beam flanges through the thickness etc. This amount of shear force can be measured corresponding to story drifts and used as a criterion to decide whether the excessive yielding of the panel zones can increase the amount of shear forces in the beam flanges.

The fractions of shear forces carried by shear tabs were obtained by calculating ratios of the shear forces over the cross sectional area of shear tab elements at the column face to the total shear forces computed from self-equilibrium of applied loads at the tip beams as shown earlier in Chapter 3. Then, these fractions were presented with corresponding story drifts.

Figure 4.4 shows the resultant shear forces carried by shear tabs of BC1 and BC16 at story drift angles of approximately 0.5%, 1%, 2%, and 4% radians. The 0.5% drift is for investigating shear force distributions when the panel zones are in the elastic stage for both weak and strong panel cases. The other drifts are assigned to observe changing of the shear force distributions when the panel zones are in the inelastic stage, and their yielding increased by a factor of 2 up to 4%. For BC16, since its panel zone is so strong, the inelastic action occurred in the beam rather than in the panel zone under those story drifts. Therefore, the shear-transfer mechanism can be used to monitor progression of the beam yielding for the strong panel zone case. As can be seen, the resultant shear force in the shear tab is almost constant approximately at 50% through out the analysis for the weak panel zone, no matter how significant yielding in the panel zone

is. It means that the remaining 50% of shear force has to be carried by the beam flanges. In the case of strong panel zone, the shear force in the beam flange is about 40% during the elastic stage. When the yielding in beam flanges spreads, these shear forces reduce to less than 10%. This result was also observed in El-Tawil's study (1998). He found that the percentage of shear transferred through the shear tab gradually increases and the distribution of shear stress changes dramatically when the yielding in the beam is in progress. Therefore, it can be concluded that spread of the inelastic action in the panel zones does not cause a significant increment of overloading shear force in the beam flanges. Instead, the spread of inelastic action in the beam flanges significantly changes the shear distribution by forcing it back into the shear tab.

Table 4.3 summarized the maximum beam bending moments at the column face of Specimens BC1 and BC16. The moments were computed by multiplying the maximum applied tip loads by the beam length, L_b. Also the values of M_p corresponding to each specimen are mentioned into the table. As can be seen, the beam of weak panel zone never reaches its expected moment. The maximum moment of this beam is approximately 27% lower than the plastic beam moment. Thus, the beam flanges and the shear tab at this location are still on the threshold of elastic range. On the contrary, the maximum moment is approximately 21% over the plastic moment for the case of strong panel zone. Since the panel zone still remained in the elastic range as shown in Figure 4.3, when the maximum moment was reached, it can be concluded that the plastic rotation of this connection came from the beam. These FE results agreed well with experiment results as mention earlier. The severe yielding of the panel zone can prevent the beam from successfully reaching its expected capability.

Figure 4.5 shows tensile stress, S11, distributions through thickness of the beam flanges. The stresses are presented in three layers (bottom, middle, and top) of the beam flanges. The tensile stresses of an additional model, BC4, were added to the existing models, BC1 and BC16. The distributions were selected at 1% drift, in which the

connections were still in the elastic range, and 4% drift, in which the connections performed in the inelastic range. It should be kept in mind that Specimen BC1 has the weakest panel zone strength compared with the stronger panel zone of BC4 and the strongest of BC16.

Under the elastic performance, the stress distribution patterns in the bottom layer of the beam flange are significantly different from those in other two layers for BC1. This big gap of stress between layers prevents uniform yielding to progress over the cross section of the beam flange. This phenomenon is also seen in the stronger panel zone specimens, but it tends to get smaller when the panel zones get stronger. The non-uniform stress distributions of the beam flanges are caused by the overloading of the shear force in this region as mention earlier. As shown in Chapter 3, the additional shear force can increase the magnitude of tensile stress in the top half, and can decrease the tensile stress in the bottom half of the beam flanges. Therefore, greater the shear force, greater is the stress difference.

Under inelastic performance, the stress distribution patterns are similar to those in the elastic stage. The gaps between stresses in the top and middle layers are close, but still wide open for the bottom and middle layers, especially in the weakest panel zone specimen. The additional shear force is also the explanation for this behavior. Most parts of the beam flanges and shear tab at the interface area of BC1 are in the elastic range at 4% drift, while other specimens have these areas under the inelastic response. Thus, BC1 has more shear forces imposed in the beam flanges than the others. Moreover, the magnitude of shear forces gets smaller when the panel zone gets stronger. Therefore, more uniform yielding of beam flanges should be expected in the stronger panel zone specimens.

In conclusion, the non-uniform tensile stress distributions in the beam flanges are developed from the additional shear force in the flanges at the interface area of the connections. The actual stress on the top surface can be considerably larger than the

design stress, while the opposite is true for the bottom surface. Thus, a crack is usually initiated in the top surface rather than in the bottom surface as observed from the tests at the column face, and the opposite is true at the tip of access hole area. The magnitude of this shear force is mainly related to the degree of yielding of the beam flanges, and it does not significantly influence by the level of yielding in the panel zone. In other words, weak panel zone can keep the beam in the elastic range; therefore, it is the beam flanges, which is more likely to suffer from the shear force. However, it does not mean that excessive yielding of panel zone can increase the magnitude of the shear force in the flanges.

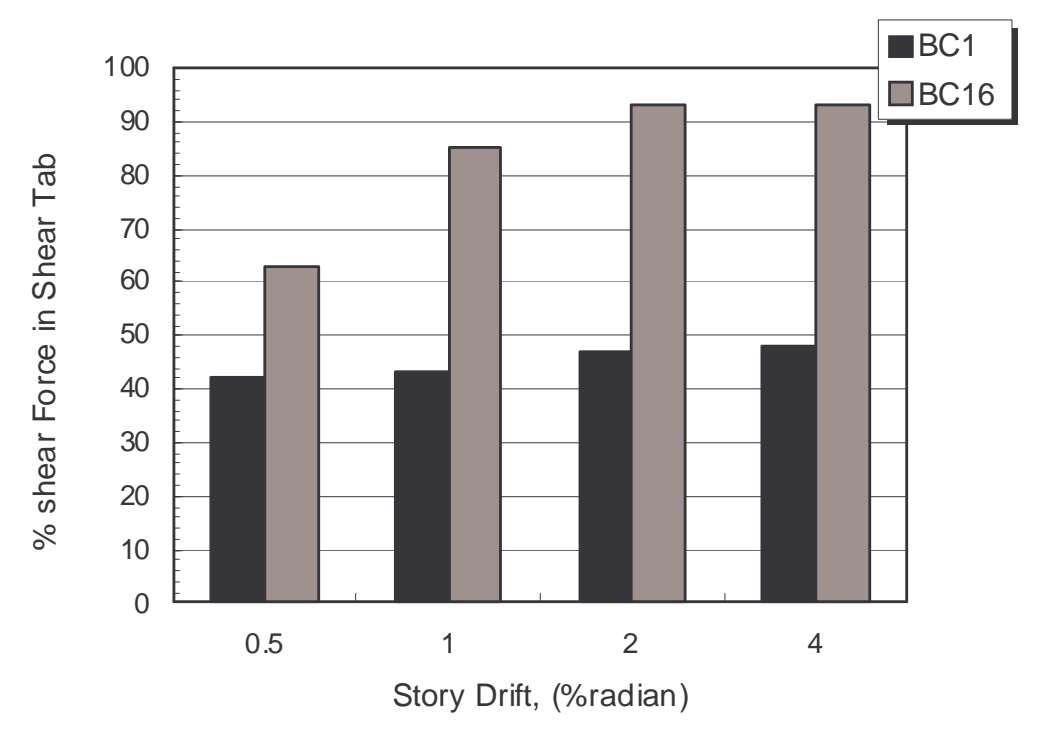


Figure 4.4. Shear forces carried by shear tabs at the different story drifts.

Table 4.3. Comparison of the maximum beam bending moments.

Specimen	Beam Bending Moment at the Column Face (kip-in.)		
	FEM.	M_{p}	% Different
BC1	16200	21840	-27%
BC16	18900	15600	21%

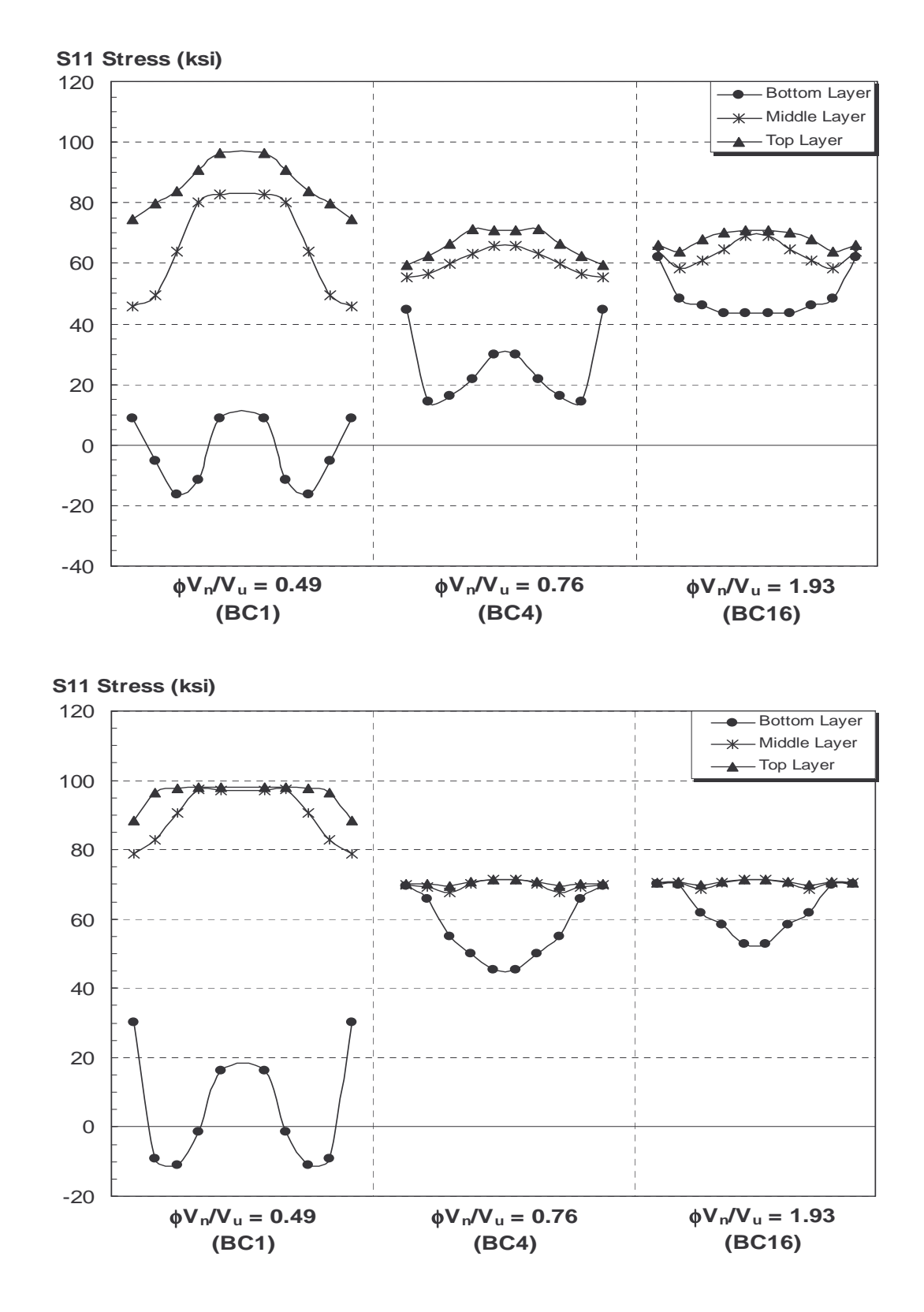


Figure 4.5. Tensile stress distributions on beam flanges at the interface area of 1% and 4% story drifts, respectively.

4.4.4 Appropriate Degree of Yielding in Panel Zones

As can be seen, the shear force in the beam flange is very important and can be used for identifying the appropriate degree of yielding in the panel zone. The amount of shear forces carried by the beam flanges are presented in terms of ratios of the shear strength and shear demand of panel zones ($\phi_v V_n / V_u$). The intention was to demonstrate the amount of shear force remaining in the beam flanges for the different panel zone strength ratios and the different yielding levels of connections. The yielding of the connections was computed at four levels of story drifts: 0.5% (elastic), 1%(just yielded), 2%(moderate yielded), 4%(fully yielded and strain hardening).

The $\phi_v V_n / V_u$ plotted against percentage of the shear force carried by the beam flanges (%V) from the study models (BCs series) is presented in Figure 4.6 by the solid dots. The solid lines are created to estimate the %V values between the data by interpolation. Regardless of their inelastic response difference, the results show that the % V can be separated into two categories: $\phi_v V_n / \ V_u$ less than 1.0 and $\phi_v V_n / \ V_u$ more than 1.0. When $\phi_v V_n / \ V_u$ is more than 1.0, the %V is very much constant. There is no significant change in the magnitude of shear force carried by the beam flanges. In other words, the amount of shear force is unaffected by the shear strength ratio or the inelastic response of the connections when $\phi_v V_n / V_u$ is more than 1.0. On the other hand, the %V is considerably sensitive to the strength ratios that are less than 1.0. Especially when panel zone has shear strength approximately less than 75% of its demand, the %V increases between 10% to 40%, depending on the stages of connection responses. This leads to an important finding that in the case of very weak panel zone ($\phi_v V_n / \ V_u < 0.75$) the shear force carried by the beam flanges is insensitive to the amount of inelasticity in the panel zone compared to the fairly weak to strong panel zone ($\phi_v V_n / \ V_u > 0.75$). For instance, the % V is approximately high at 50% to 60% for BC1 ($\phi_v V_n / V_u = 0.49$) no matter how much is the inelastic response of the panel zone. But, the %V rapidly decreases from 50%

to 20% for BC4 ($\phi_v V_n / V_u = 0.76$) when the yielding of panel zone starts to spread (panel zone rotation increases from 0.5% to 2% story drifts). Thus, based on these results, it can be concluded that, for a very weak panel zone connection, spreading of the inelasticity in the panel zone can cause a stress condition at the interface region more critical than the same situation in fairly weak to strong panel zone connections.

From the design point of view, the panel zones can be classified into three types according to the values of $\phi_v V_n / V_u$. A relatively very weak panel zone ($\phi_v V_n / V_u < 0.75$) can have a the detrimental influence on the connections. Even though very weak panel zone can be an excellent source of energy absorption, the connection can be damaged in rather undesirable modes such as fracture in the beam flanges or in the column k-zone. The fairly weak panel zone (0.75 < $\phi_v V_n / V_u < 1.0$) should be considered as a better choice in the new panel zone design, because the connections have high probability to meet both ductility and strength requirements. The strong panel zone ($\phi_v V_n / V_u > 1.0$) should be used only with the new connection types where the beam is capable to produce all the needed plastic rotation.

%Shear Force in Beam Flange

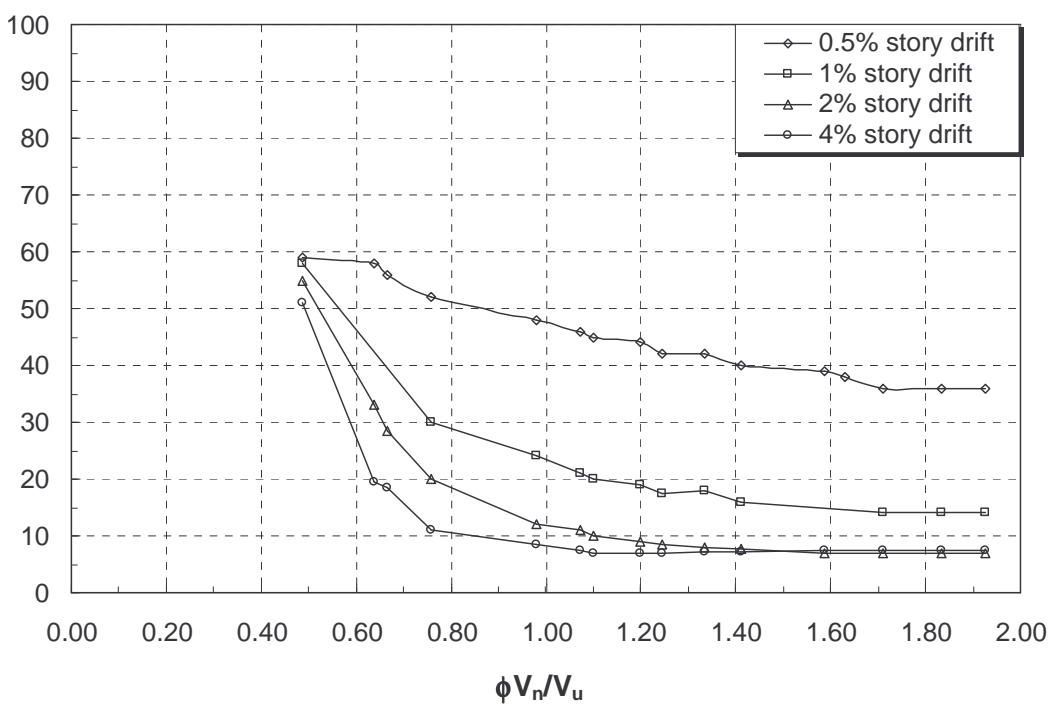


Figure 4.6. % shear forces carried by the beam flanges vs. shear strength ratios of the panel zones at approximately 0.5%, 1%, 2%, 4% story drifts.

CHAPTER 5

SUMMARY AND CONCLUSIONS

5.1 SUMMARY AND CONCLUSIONS

The behavior of steel moment connections was intensively studied in respect to panel zone parameter. The study focused on answering the questions: how this element contributes to ductility and fracture of the connections and how it should be appropriately designed. The objectives of this study were achieved by investigating the results from the finite element analyses of exterior connections subjected to monotonic and cyclic loading. Based on the finite element analysis studies, the major findings are summarized in the following sections.

- 1) The results from finite element analyses showed that the stress distributions near the connections are very complex. The beam flange in this region is not only subjected to a high tensile stress, but also subjected to considerable shear stresses through its thickness. The region most vulnerable to fracture is the area between the column face and the beginning of the weld access hole.
- 2) The shear stress distribution in the connection area is in contradiction to the assumption made in the classical beam theory. Here, most of the shear force is carried by the beam flanges instead of the web. This additional shear force causes non-uniform stress distribution across and through thickness of the beam flanges, which can lead to fracture before uniform yielding of beam flanges can occur.
- 3) The shear stress in the shear tab of the connection is locally concentrated in the corners of the shear tab, with little or no shear stress in the middle portion of the shear

tab. This study suggests that the effective height of the shear tab can be taken as approximately two-thirds of the total height of conventional shear tab for carrying the shear force in this area.

- 4) The finite element models including types of elements, monotonic loading, and strain hardening assumptions etc., developed in this study were validated with the test results and can be used to perform the connection parametric study.
- 5) The weak panel zone connection specimens showed that the panel zones demonstrate considerable reserve strength beyond the elastic range without strength degradation of connections, and no local kinks were observed in the column flanges. Their hysteretic responses are quite stable with excellent energy absorption. It can be concluded that the panel zone deformation can be beneficial to some degree. An appropriate limit should be assigned in order to get a balanced inelastic response between the panel zone and beam.
- 6) The amount of shear force carried by the beam flanges can be effectively used as a parameter to measure potential of the connection fracture. Low shear force can lead to uniform yielding over the beam flange thickness and reduce the potential of flange fracture.
- 7) The ratio $(\phi_v V_n/V_u)$ of shear capacity (Equation 4.2) and shear demand (Equation 4.1) of panel zones with the assumption of beam moment of M_p at the column face can successfully determine the degree of inelasticity in the panel zones for the post-Northridge connection. Panel zones with $\phi_v V_n/V_u < 0.75$ can be categorized as a very weak panel zone, $0.75 < \phi_v V_n/V_u < 1.0$ as a fairly weak panel zone, and $\phi_v V_n/V_u > 1.0$ as a strong panel zone. Excessive yielding of the panel zones should be expected in the connections that have $\phi_v V_n/V_u$ less than 0.75, and can cause serious stress conditions in the beam flanges.
- 8) Spread of inelasticity in a very weak panel zone can cause high shear forces in the beam flanges, and eventually can increase the potential of their brittle fracture. On

the other hand, the amount of shear force reduces to less than one-third when inelasticity propagates in the fairly weak and strong panel zones.

5.2 SUGGESTIONS FOR FUTURE STUDIES

- 1) The finite element study should be extended to the interior moment connections.
- 2) Inelastic response of panel zones substantially depends on the accurate calculation of their shear capacity (V_n) and shear demand (V_u) . Nevertheless, this preliminary study clearly shows that the equations used in current practice and procedures for computing the shear capacity (V_n) , and shear demand (V_u) of the panel zones do not give reliable results, especially with new moment connection types. Therefore, a new design procedure needs to be established, which should include a new mathematical model to predict the shear strength of the panel zones and a reliable value of shear demand calculated from the beams.
- 3) The proposed design concept of balance yielding of panel zone need to be verified with the experimental study.

REFERENCES

- 1. ABAQUS (1997), "User's Manual I-VI Version 5.7", Hibbit, Karlsson, and Sorenson, Inc, 1080 Main Street, Pawtucket, RI 02860.
- 2. American Institute of Steel Construction (1994), "Load and Resistance Factor Design Specification for Structural Steel Buildings", AISC, 2nd Edition, Chicago, Illinois.
- 3. American Institute of Steel Construction (1997), "Seismic Provisions for Structural Steel Building", AISC, Chicago, Illinois.
- 4. American Institute of Steel Construction (2000), "Seismic Provisions for Structural Steel Building", AISC, Chicago, Illinois.
- 5. American Institute of Steel Construction (2005), "Prequalified Connections for Special and Intermediate Steel Moment Frames for Seismic Applications", AISC, Chicago, Illinois.
- 6. American Institute of Steel Construction (2005), "Seismic Provisions for Structural Steel Building", AISC, Chicago, Illinois.
- 7. Bertero, V.V., Popov, E.P., and Krawinkler, H. (1972), "Beam-Column Subassemblages under repeated loading." Journal of Structural Engineering, ASCE, 98(5), pp. 1137-1159.
- 8. Bertero, V.V., Anderson, J.C., and Krawinkler, H. (1994), "Performance of Steel Building Structures During the Northridge Earthquake", Technical Report UCB/EERC-94/09, Earthquake Engineering Research Center, Univ. of California, Berkeley, California.
- 9. Chen, S.J., Yeh, C.H., and Chu, J.M. (1996), "Ductile Steel Beam-to-Column Connections for Seismic Resistance", Journal of Structural Engineering, ASCE, Vol. 122, No. 11, November, pp. 1292-1299.
- 10. Deierlein, G.G. (1998), "Summary of SAC Case Study Building Analyses", Journal of Performance of Constructed Facilities", Vol. 12, No. 4, November, pp.202-212.
- 11. El-Tawil, S., Mikesell, T., Vidarsson, E., and Kunnath, S. (1998), "Inelastic Behavior and Design of Steel Panel Zones", Journal of Structural Engineering, ASCE, Vol. 125, No. 2, pp. 183-193.
- 12. El-Tawil, S., Vidarsson, E., Mikesell, T., and Kunnath, S. (1999), "Strength and Ductility of FR Welded-Bolted Connections", Report No. SAC/BD-98/01, SAC Joint Venture, Sacramento, California.

- 13. Engelhardt, M. D., and Husain, A. S. (1993), "Cyclic-Loading Performance of Welded Flange-Bolted Web Connections", Journal of Structural Engineering, ASCE, Vol. 119, No. 12, pp. 3537-3549.
- 14. Englehardt, M.D., and Sabol, T.A. (1994), "Testing of Welded Steel Moment Connections in Response to the Northridge earthquake", Progress Report, AISC Advisory Subcommittee on Special Moment Resisting Frame Research.
- 15. Englehardt, M.D., and Popov, E.P. (1998), "Cyclic-Loading Performance of Welded Flange-Bolted Web Connections", Journal of Structural Engineering, ASCE, 119(12), pp. 3537-3549.
- 16. Federal Emergency Management Agency (1995), "Interim Guidelines: Evaluation, Repair, Modification and Design of Welded Steel Moment Frame Structures", Report FEMA-267, SAC Joint Venture, Sacramento, California.
- 17. Federal Emergency Management Agency (1997), "Interim Guidelines advisory No. 1", Report No. SAC-96-03, SAC Joint Venture, Sacramento, California.
- 18. Federal Emergency Management Agency (2000), "Recommended Seismic Design Criteria for New Steel Moment-Frame Buildings", Report FEMA-350, SAC Joint Venture, Sacramento, California.
- 19. Fielding, D.J., and Huang, J.S. (1971), "Shear in Steel Beam-to-Column Connections", Journal of Welding Research Supplement, July, pp. 313s-326s.
- 20. Goel, S.C., and Stojadinovic, B., and Lee, K.H., Margarian, A.G., Choi, J.H., Wongkaew, A., Reyher, B.P., and Lee, D.Y. (1998), "Conduct Parametric Tests of Unreinforced Connections", Preliminary Report to SAC, Task 7, Subtak 7.02, Unv. of Michigan, Ann Arbor, Michigan.
- 21. Huang, J.S., Chen, W.F., and Beedle, L.S. (1973), "Behavior and Design of Steel Beam-to-Column Moment Connections", Welding Research Council, Bulletin 188, pp. 1-23.
- 22. Krawinkler, H. (1978), "Shear in Beam-Column Joints in Seismic Design of Steel Frames", Engineering Journal, AISC, Vol. 15, No. 3, pp. 82-91.
- 23. Krawinkler, H., Bertero, V.V., and Popov, E.P. (1975), "Shear Behavior of Steel Frame Joints", Journal of the Structural Division, ASCE, Vol. 101, No. ST11, pp. 2317-2335.
- 24. Krawinkler, H., and Mohasseb, S. (1987), "Effects of Panel Zone Deformation on Seismic Response", Journal of Constructional Steel Research, Vol. 8, pp. 233-250.

- 25. Lee, K.H., Goel, S.C., and Stojadinovic, B. (1997), "Boundary Effects in Welded Steel Connections", Report UMCEE 97-20, Dept. of Civ. & Env. Engrg., Unv. of Michigan, Ann Arbor, Michigan.
- 26. Popov, E. P., and Bertero, V.V. (1973), "Cyclic Loading of Steel Beams and Connections", Journal of Structural Engineering, ASCE, Vol. 99, No. ST6, June, pp. 1189-1204.
- 27. Popov, E.P., Bertero, V.V., and Chandramouli, S. (1975), "Hysteretic Behavior of Steel Columns", Report EERC 75-11, Earthquake Engineering Research Center, Univ. of California, Berkeley, California.
- 28. Popov, E.P., Amin, N.R., Louie, J.C., and Stephen, R.M. (1986), "Cyclic Behavior of Large Beam-Column Assemblies", Engineering Journal, AISC, First Quarter, pp. 9-23.
- 29. Popov, E. P. (1987), "Panel Zone flexibility in Seismic Moment Joints", Journal Construction Steel Research, Barking, England, pp. 91-118.
- 30. Popov, E.P., Tsai, K-C, and Engelhardt, M.D. (1989), "On Seismic Steel Joints and Connections", Engineering Structures, Vol. 11, July, pp. 148-162.
- 31. Popov, E.P., Yang, T-S, and Chang S-P (1998), "Design of Steel MRF Connections before and after 1994 Northridge Earthquake", Engineering Structures, Vol. 20, No. 12, pp. 1030-1038.
- 32. Ricles, J.M., Mao, C., Lu, L-W., Fisher, J.W. (2000), "Development and Evaluation of Improved Details for Ductile Welded Unreinforced Flange Connections", Draft, SAC Task 7.05, April, SAC Joint Venture, Sacramento California.
- 33. Roeder, C.W., Schneider, S.P., and Carpenter, J.E. (1993), "Seismic Behavior of Moment-Resisting Steel Frames: Analytical Study", Journal of Structural Engineering, ASCE, Vol. 119, No. 6, June, pp. 1866-1883.
- 34. SAC (1996), "Experimental Investigation of Beam-Column Subassemblages: Part 1 and Part 2", Report SAC 96-01, SAC Joint Venture, Sacramento California.
- 35. SAC (1996), "Steel Connection Subassemblage: Testing Investigations, Northridge Earthquake, Report SAC 96-01, SAC Joint Venture, Sacramento California.
- 36. SAC (1995), "Analytical and Field Investigations of Buildings Affected by the Northridge Earthquake: Part 2", Report SAC 95-04, SAC Joint Venture, Sacramento California.
- 37. SAC (1999), "Connection Performance TAP Meeting", Minutes and Material from the meeting, SAC Joint Venture, San Francisco California.

- 38. Salmon, C.G., and Johnson, J.E. (1996), "Steel Structures: Design and Behavior", HarperCollins, New York, USA.
- 39. Stojadinovic, B., Goel, S., Lee, H.K., Margarian, A.G., and Choi, J.H. (2000), "Parametric Tests on Unreinforced Steel Moment Connections", Journal of Structural Engineering, ASCE, Vol. 126, No. 1, January, pp. 40-49.
- 40. Tsai, K. C., and Popov, E. P. (1990), "Seismic Panel Zone Design Effect on Elastic Story Drift in Steel Frames", Journal of Structural Engineering, ASCE, Vol. 116, No. 12, December, pp. 3285-3301.
- 41. Tsai, K. C., Wu, S., and Popov, E. P. (1995), "Experimental Performance of Seismic Steel Beam-Column Moment Joints", Journal of Structural Engineering, ASCE, Vol. 121, No. 6, June, pp. 925-931.
- 42. Wongkaew, A., Goel, S.C., and Stojadinovic, B. (2001), "Development of Improved Details for Unreinforced Welded Steel Moment Connections", Report UMCEE 01-20, Dept. of Civ. & Env. Engrg., Unv. of Michigan, Ann Arbor, Michigan.

APPENDIX

Conference Proceeding:

 Arnon W., "Behavior of Steel Moment Connections Subjected to Earthquake Loading using Finite Element Analysis", the 12th National Convention on Civil Engineering–Thailand Advances with Civil Engineering, Phitsanulok, Thailand, May 2-4, 2007.

BEHAVIOR OF STEEL MOMENT CONNECTIONS SUBJECTED TO EARTHQUAKE LOADING USING FINITE ELEMENT ANALYSIS

Arnon Wongkaew¹

Faculty of Engineering, Department of Civil Engineering, Burapha University, Chonburi, 20131

ABSTRACT: Unprecedented widespread failure of welded moment connections was observed in steel moment resisting frames caused by the 1994 Northridge and the 1995 Kobe earthquakes. The common damages came from fractures in the beam-to-column moment connection region. In this study, the finite element (FE) analyses of a typical beam-to-column moment connection subjected to lateral loading were performed to identify some potential problems of the connections. The analytical results show that the state of stresses around the connection area is, in fact, very complex. The current design practice following the classical beam theory is inadequate to meet the required strength of the connections. The beam flanges have to carry a considerable shear force instead of the shear tab. This shear force can cause premature fracture of the beam flanges.

KEYWORDS: Steel Moment Connection, Finite Element (FE) Analysis, Fracture, Shear Force

1. Introduction

Moment resisting structure steel frames have long been recognized as one of the best structural systems to resist seismic forces. The performance of such frames under seismic forces depends primarily on the strength and ductility of their beam-to-column connections and bracing systems. These frames are intentionally designed such that seismic energy imparted to the frames can be dissipated by yielding of the material near moment connections. In other words, safety of such structures depends mainly on capability of the structures to absorb energy in the inelastic range rather than on the elastic stiffness of the structures. However, widespread damage of welded moment connections in the moment-resisting steel frames was reported after the 1994 Northridge Earthquake in the US and the 1995 Kobe Earthquake in Japan. It has undermined confidence in the ductility of the moment resisting frames, and raised many questions regarding the validity of existing design and construction procedures for moment connections. After, earthquakes, many extensive research programs were funded by several agencies in order to gain a better understanding of steel moment connections behavior and performance.

The overall objective of this paper is to more closely examine the behavior of welded-bolted moment connections, especially in the interface region between the column face and the beam end. Specific goals of this study are to (1) gain a better understanding of both elastic and inelastic behavior of the connection area; (2) investigate the flow of forces and stresses in the connection area; (3) examine the role of shear force distribution on the potential of fracture of the connection; (4) investigate the effect of the column strength to the shear distribution in the connection area. These

objectives are addressed through detailed nonlinear finite element analyses of steel welded-bolted exterior moment connections.

2. Analysis Configurations

Based on available experimental data, the geometries of the analysis configurations utilized in this research are derived from the geometry of specimens tested at the University of Michigan, Ann Arbor during Phase II of the SAC steel project. These particular specimens are representative of the exterior moment connection extensively constructed before the Northridge earthquake.

Figure 1 shows a test setup of the connection specimens. The span length between the center of actuator to the face of column is 134 inches, and the distance between the supports is 144 inches. The configurations that are analyzed in this work are shown in Table 1 (detail dimensions can be seen in AISC-LRFD specification [2]). As can be seen from the table, the beams were kept to the same size for all 3 specimens with W30x99, but the column sizes were varied by increasing from W14x145 to W14x257. It obviously suggests that SP4 has weaker column strength than SP5, and SP6 has the strongest of all 3 specimens. It should be noted that these 3 specimens were designed to satisfy the strong column-weak beam requirement according to AISC-LRFD 1997.

Table 1 Specimen Configurations Analyzed in the Study

Specimen	Column	Beam
SP4	W14x145	W30x99
SP5	W14x176	W30x99
SP6	W14x257	W30x99

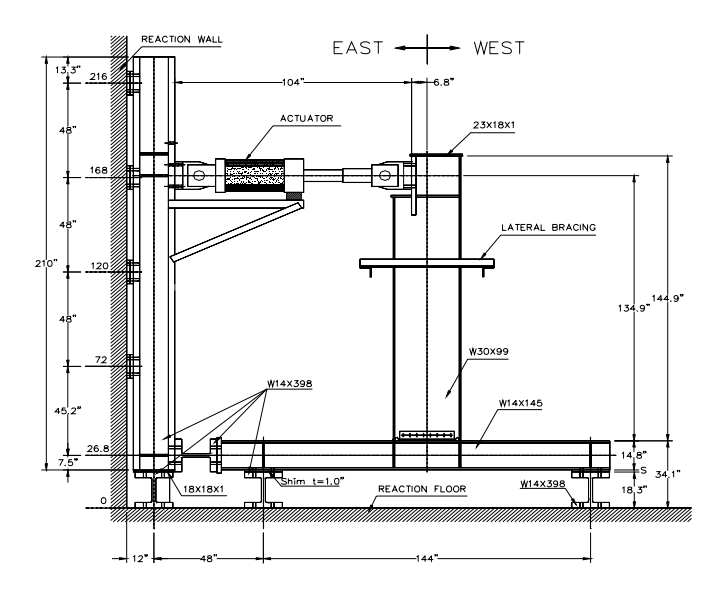


Figure 1 Test set-up [8, 9]

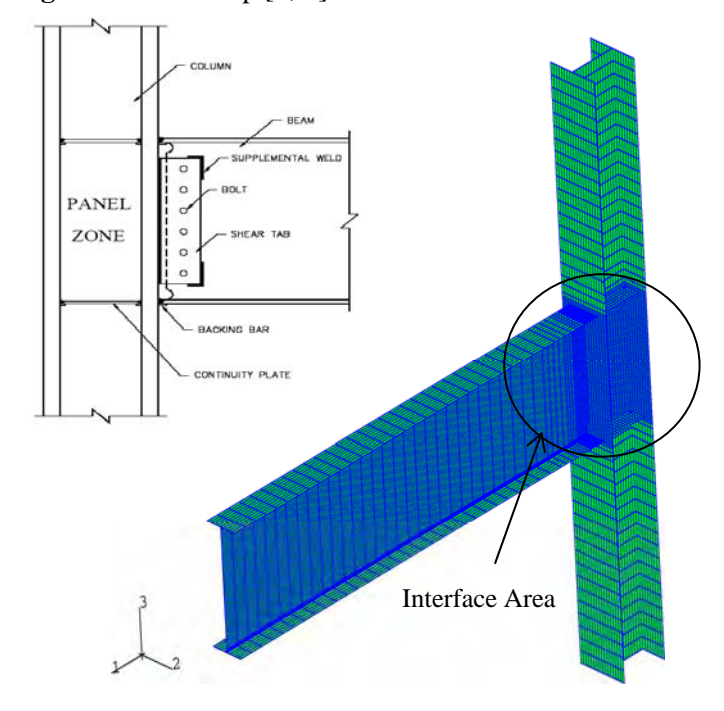


Figure 2 Finite element model

3. Finite Element Model

The general-purpose finite element analysis program ABAQUS was used to develop 3-D models of moment connections. The finite element model used in this study was composed of four-node shell elements (S4R). Although local and through-thickness behavior can not be accurately computed using the shell element, the S4R element provides outputs of the stress distributions as layers and transverse shear stress through the element thickness. Figure 2 shows the finite element model of a particular exterior connection. Multipoint constraints were applied to all connected interfaces between the webs and the flanges, the continuity plates and the flanges, the shear tabs and the webs, and the shear tabs to column flanges. It should be noted that the welds, bolts, and backing bars were not modeled. The

support condition at the column ends was modeled as a pin boundary condition by allowing a free rotation, but restrained the in-plane and out-of-plane displacement. The finite element models were subjected to both elastic and inelastic analysis. However, only material non-linearity of the connections was included in the inelastic analysis.

For the elastic analysis, beams, columns, shear tabs, continuity plates were assumed to have an elastic modulus of 29,000 ksi. The load was applied at the tip of the beams as a monotonic increasing static force as maximum as 100 kips. For the inelastic analysis, the material of beams, columns, shear tab, continuity plates were assumed to be A527 Grade 50 steel. The steel has an assumed yield strength of $F_v = 50$ ksi. with elastic modulus of 29,000 ksi. The steel was also assumed to have strain hardening modulus equal to 5% of the elastic modulus up to 1% strain. The steel was assumed to be perfectly plastic for larger strains. Differences between the base metal and weld metal properties were disregarded. The inelastic analysis was conducted by applying monotonically increasing static displacement at the beam tip to a maximum of 6 inches (4% story drifts).

4. Verification of Finite Element Model

In order to verify global behavior of the connection, a comparison between analytical and experimental results for specimen SP4 tested at the University of Michigan, Ann Arbor is shown in Figure 3. The analysis was done following the nonlinear analysis guidelines[6]. The load-displacement response of the connection shows good agreement between the analysis and the experiment. The initial yield load is 80 kips and 85 kips for the test and analysis, respectively. The corresponding displacement is approximately 1.4 inches and 1.5 inches, respectively. The maximum load at 5.5 inches displacement is 116 kips and 115 kips for the test and analysis, respectively.

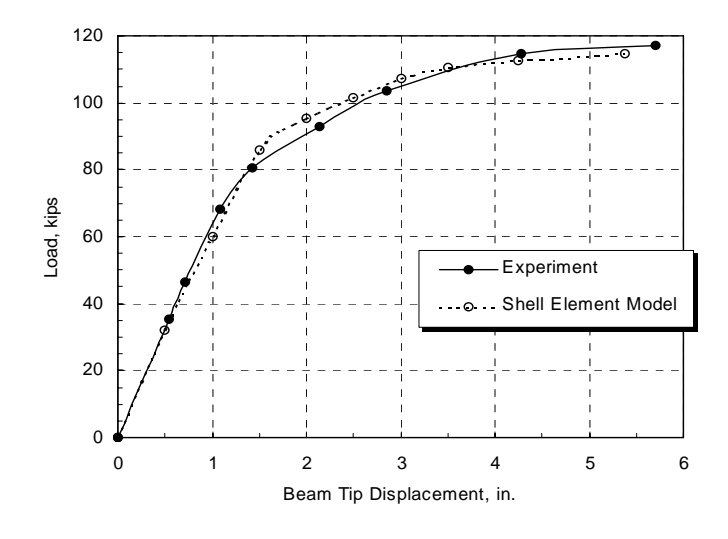


Figure 3 Comparison of load-displacement responses between test and FE result of SP4

5. Elastic Analysis Results of SP4

Figure 4 and 5 present the principal stress vector and von Mises stress distribution in the connection region. The vector plot shows a heavy concentration of the principal stresses flowing through the beam flange connected to the column flange. Also from Figure 5 and 6, the highest value of von Mises stress is at the center of the beam flange in a very limited region at the junction of the beam flange and the column flange. This result implies that the possibility of brittle fracture in this region is much higher than elsewhere in the connection interface area. Further investigation is made by plotting von Mises stress distributions in the beam flange at the column interface as shown in Figure 6. Through thickness of the beam flange was represented by three layers, top, middle, and bottom. The maximum values occur at the middle of the beam flange. The stress rapidly decreases toward the edges for all layers. In addition, the stress gradient between the top and bottom layer of the beam flange is significantly large. This gradient can cause non-uniform yielding of the beam flange. Since this non-uniform yielding occurs in a very restricted area surrounding by still elastic and stiff material, this condition can prevent the spread of yielding out further to the flange and into the beam web. Such restrained stress state may be a reason for beam flange brittle fracture instead of ductile yielding. Moreover, the stress distribution from the analysis is fundamentally different from the results assuming from the classical beam theory which is a uniform distribution across the beam width as shown with the solid line.

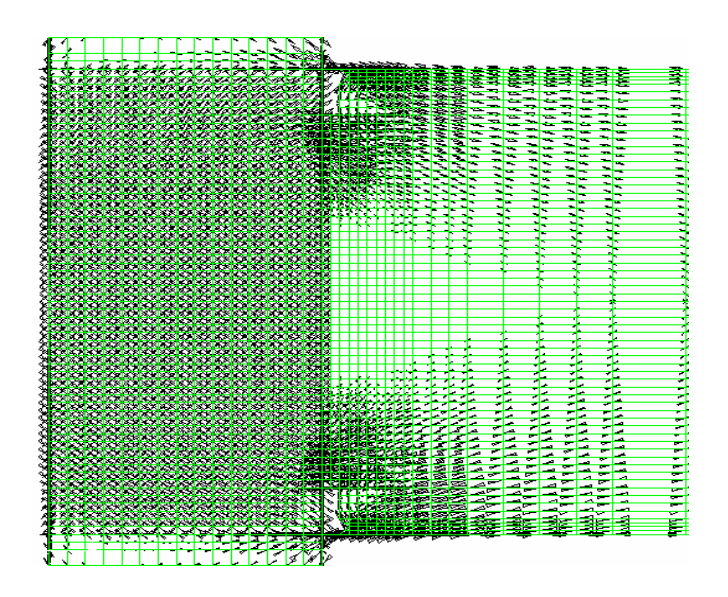


Figure 4 Principal stress vectors in the connection area

The shear stress from the FE model was plotted in Figure 7 against the depth of shear tab. The y-axis represents the height of the shear tab measured from the neutral axis of the beam. The thin solid line shows the shear stress distribution computed using the FE model. The thick solid line represents the distribution obtained from the beam theory. As can be seen, the highest shear

stress in the FE model did not occur at the neutral axis, as it was expected by the beam theory. In contrast, the highest stress occurred close to the corners of the shear tab. This phenomenon is caused by the boundary effect in beam-to-column connection [9].

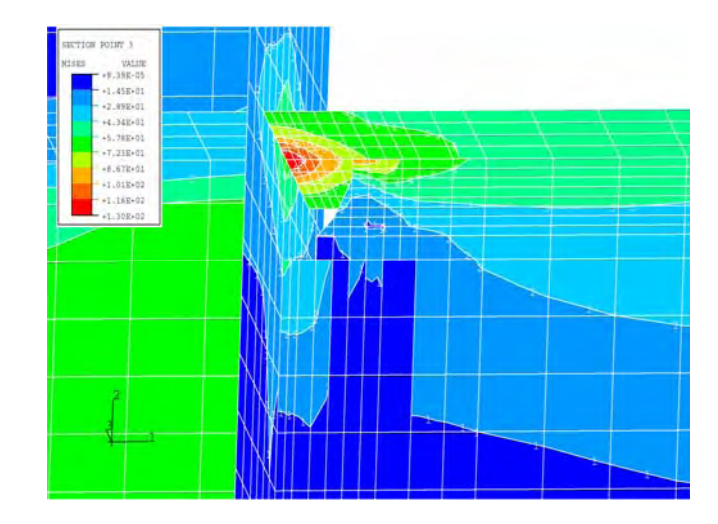
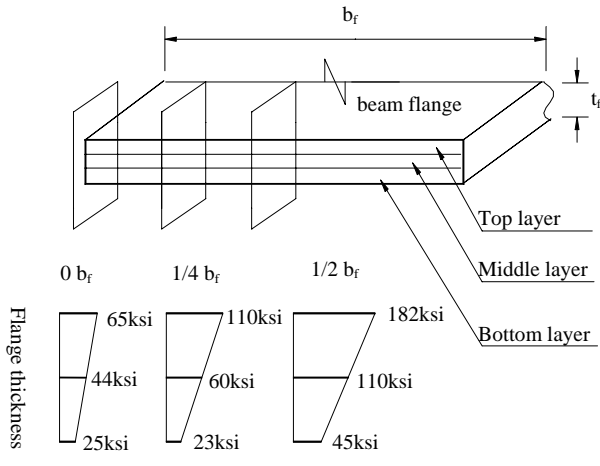


Figure 5 von Mises stress distributions in the connection area



Through thickness Mises stress (bf=beam flange width)

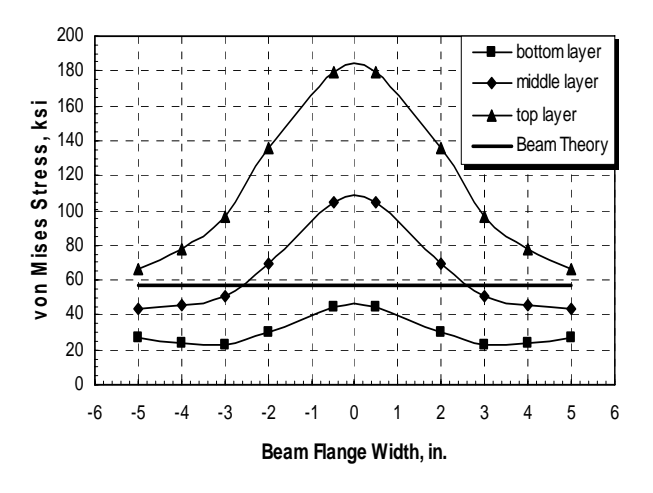


Figure 6 von Mises stress distributions on the beam flange

To reinforce this result, fractions of the shear force carried by the shear tab and the beam flanges were computed by summing up the shear stress in the interface cross section. This calculation can be approximated by summing up products of the average element shear stress in each element and element cross-sectional area along the considered section. The shear force carried by the shear tab is 34 kips, computed from the plot in Figure 7. Since the applied force was 100 kips, the remaining of 66 kips has to be carried by the beam top and bottom flange. It can be seen that the beam flanges can be overloaded by this unexpected shear force. The same calculation of the shear distribution is performed for the cross-section of the beam web at 30 inches away from the interface area. The shear force in the beam web is about 97 kips. Thus, the flanges carry approximately 3 kips of shear force. This shows that the beam theory is applicable at distances away from the interface area of the connections, but not at the interface area.

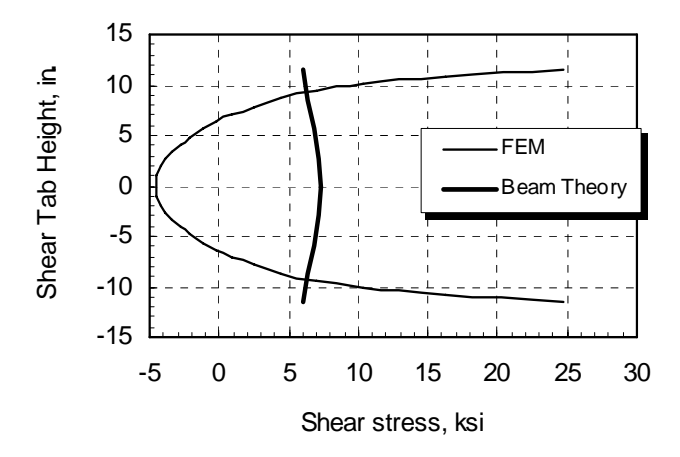


Figure 7 Shear stress distributions in the shear tab, 0.25 in. from the column face.

6. Inelastic Analysis Results of SP4

Figure 8 shows contours of shear and von Mises stresses in the plane of the beam and column webs at the incremental loading of 6.0 inches displacement. The yielding initiated from the center of column panel zone and propagated toward the corners of the column panel zone and the column flanges. The maximum shear stress in the column panel zone was 36 ksi. for almost the whole area of the column web. However, shear stress decreased rapidly to almost zero directly beneath continuity plates. The direction of the shear stress in the column web changes under the continuity plates. The maximum von Mises stress was approximately 62 ksi, where the yield stress of this FE model was set at 50 ksi. During the column panel zone yielding, the beam flanges started to yield within a limited area. Minimal yielding was observed near the weld access hole and in the beam web. This shows that the beam never reached its fully plastic stage. The stress contours and yield mechanisms of the column panel zone and around the connection area obtained from the FE analysis were similar to what had

been observed from the tested Specimen 4 as shown in Figure 9. The column panel zone completely yielded over the entire web area, and the minimum yielding occurred in the connection area, around the weld access hole and the beam web.

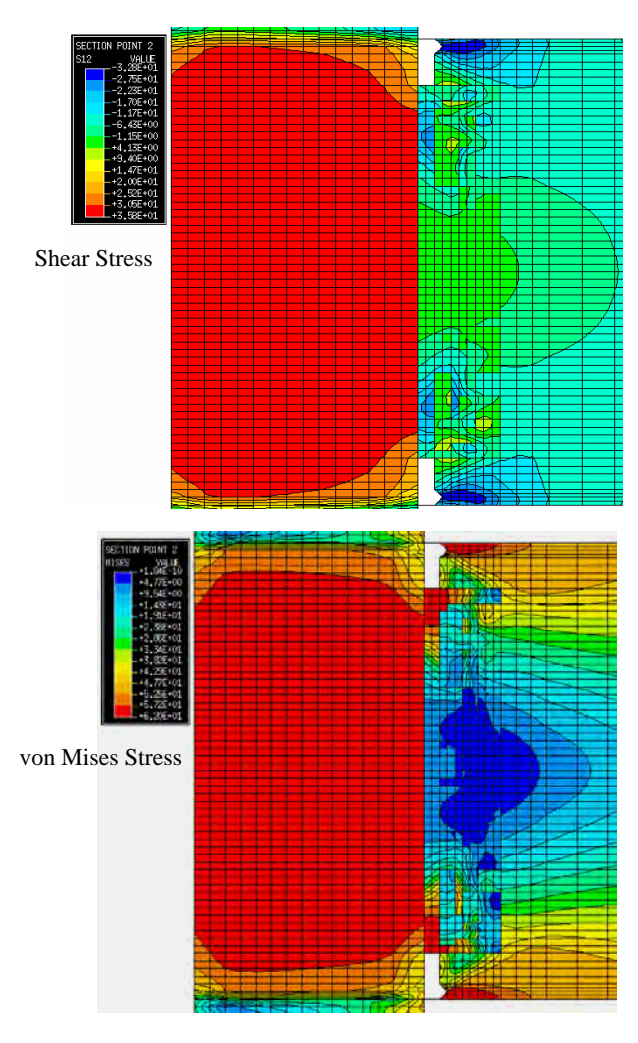


Figure 8 Shear stress and von Mises stress contours for SP4

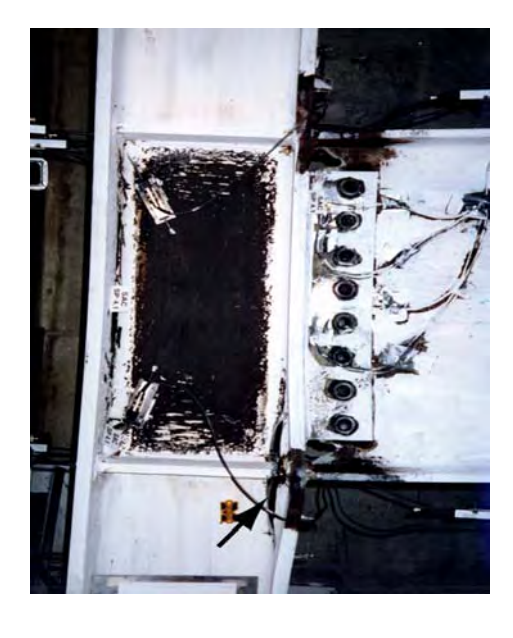


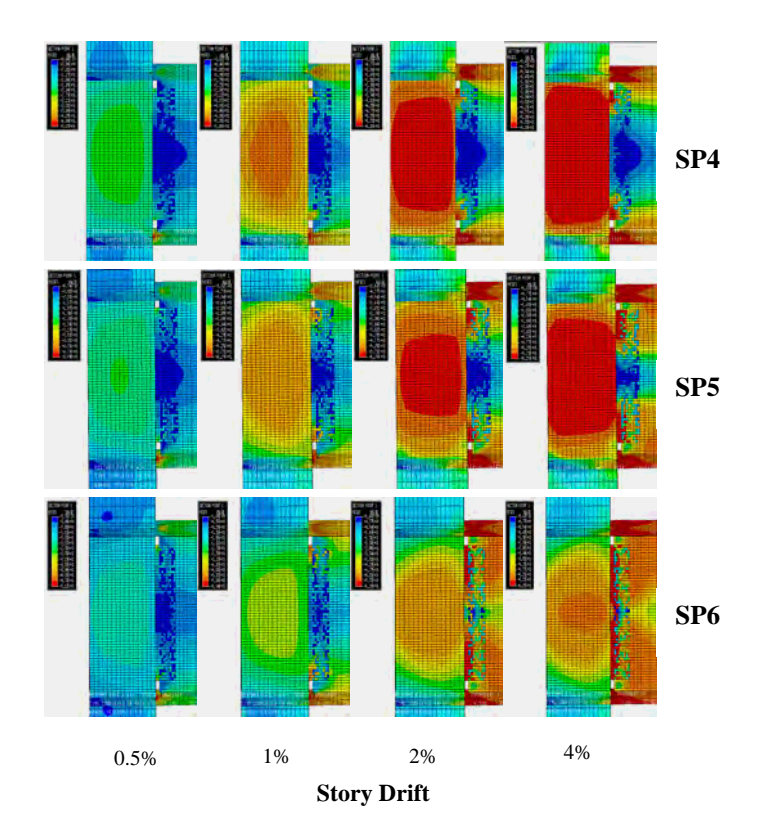
Figure 9 A photo of test Specimen 4 [8]

7. Results on Influence of Column Strength to Shear Distribution at Connection Interface Area

As mentioned, the shear stress distribution at the connection area does not follow the shear stress distribution predicted by the beam theory. The additional shear stress is redistributed from the shear tab into the beam flanges. This additional shear stress can impose as a shear force carried by the beam flanges. The amount of this overlooked shear force can be significantly large. Thus, the beam flange would be overloaded, in which it can lead to premature failures. Nevertheless, the previous conclusion was made entirely on the elastic behavior of the connection. For this part of the study, the inelastic behavior of the connections is considered. Moreover, the relative strength between the column and beam is also included by increasing the size of the column and keeping the size of the beam about the same as shown in Table 1.

When the inelastic behavior of the connection progresses, the amount of shear force can be measured corresponding to story drifts and used as a criterion to decide whether the excessive yielding of the columns can increase the amount of shear forces in the beam flanges. The fractions of shear forces carried by shear tabs were obtained by calculating ratios of the shear forces over the cross sectional area of shear tab elements at the column face to the total shear forces computed from self-equilibrium of applied loads at the tip beams as shown earlier. Then, these fractions were presented with corresponding story drifts.

Figure 10 shows the resultant shear forces carried by shear tabs of SP4, SP5, and SP6 at story drift angles of approximately 0.5%, 1%, 2%, and 4% radians. The 0.5% drift is for investigating shear force distributions when the connections are in the elastic stage for both weak and strong column cases. The other drifts are assigned to observe changing of the shear force distributions when the connections are in the inelastic stage, and their yielding increased by a factor of 2% up to 4%. Since SP4 has weakest column strength, the inelastic action of the connection mainly concentrated in the column panel On the other hand, SP6 has strongest column strength, the inelastic action occurred in the beam rather than in the column panel zone under those story drifts. For SP4, the resultant shear force in the shear tab increases from 45% to 70%, when story drift increases from 0.5% to 4%, respectively. Similarly, SP5 and SP6 have the same trend as SP4 for the shear distribution. The difference is the amount of shear carried by shear tab. When the column strength is increased, the amount of shear in shear tabs also increases. In the case of SP5, the shear force in the shear tab is 50% during the elastic stage. However, when the yielding in beam flanges spreads, these shear forces approximately increase by 20%. The same trend of the shear force distribution is also observed for SP6. This phenomenon can be explained as the percentage of shear transferred through the shear tab gradually increases and the distribution of shear stress changes dramatically when the yielding in the beam is in progress from flange to web and shear tab. Therefore, it can be concluded that spread of the inelastic action in the column panel zones does not cause a significant increment of overloading shear force in the beam flanges. Instead, the spread of inelastic action in the beam flanges significantly changes the shear distribution by forcing it back into the shear tab.



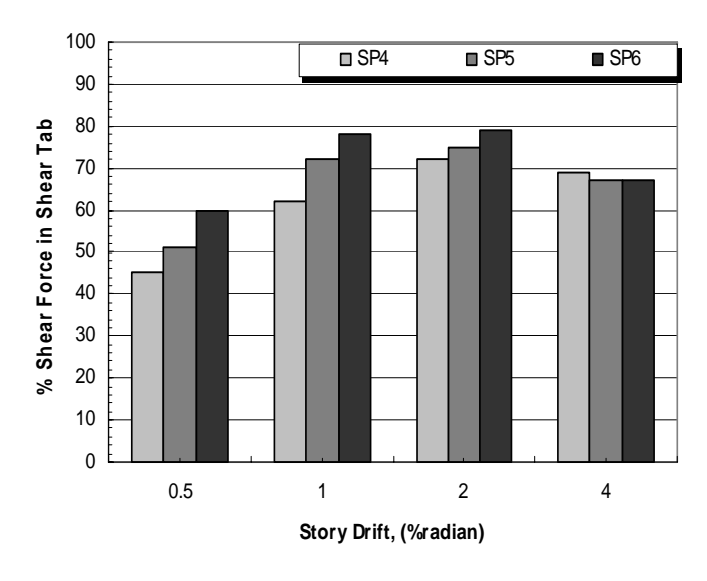


Figure 10 Shear forces carried by shear tabs at the different story drifts

8. Conclusions

Detailed finite element analyses were conducted to study the behavior of steel moment connections both elastically and inelastically. The comparisons between the test and finite element analyses indicated that the finite element models developed in the study, which include types of elements, model assumptions, monotonic loading, strain hardening etc., are quite accurate and can be used to perform the connection parametric study. The FE analyses showed that the stress distributions near the connections are much more complex than what are usually assumed in designs. The von Mises stress is critical at the center of the beam flange, and at the weld to the column flange. The results also showed that the beam flanges are not only subjected to high stresses, but it is also subjected to considerable shear stress over thickness of the flanges. The multi-axial stress and relatively high stress intensities can be one of the reasons causing early flange fractures in the pre-Northridge connections. The most vulnerable region is the area between the column face and the beginning of the weld access hole.

The column panel zone yielding does not have crucial influence to the distribution of shear stress in the beam flange at the interface area. Instead, the spreading of yielding in the beam flange significantly reduces the amount of shear force carried by the beam flange. Since the shear force is forced back into the shear tab, when the inelastic action in the beam flange is in progress.

9. Acknowledgement

The author would like to acknowledge the financial support provided by Faculty of Engineering at Burapha University through grant number 5/2549 and partially form Thailand Research Fund through grant number MRG4780220. The experimental data used in this study was obtained from University of Michigan with much appreciation.

10. References

- [1] ABAQUS (1997), "User's Manual I-VI Version 5.7", Hibbit, Karlsson, and Sorenson, Inc, 1080 Main Street, Pawtucket, RI 02860.
- [2] American Institute of Steel Construction (1994), "Load and Resistance Factor Design Specification for Structural Steel Buildings", AISC, 2nd Edition, Chicago, Illinois.
- [3] American Institute of Steel Construction (1997), "Seismic Provisions for Structural Steel Building", AISC, Chicago, Illinois.
- [4] American Institute of Steel Construction (2000), "Seismic Provisions for Structural Steel Building", AISC, Chicago, Illinois.
- [5] El-Tawil, S., Mikesell, T., Vidarsson, E., and Kunnath, S. (1998), "Inelastic Behavior and Design of Steel Panel Zones", Journal of Structural Engineering, ASCE, Vol. 125, No. 2, pp. 183-193.
- [6] Federal Emergency Management Agency (1995), "Interim Guidelines: Evaluation, Repair, Modification and Design of Welded Steel Moment Frame Structures", Report FEMA-267, SAC Joint Venture, Sacramento, California.

- [7] Federal Emergency Management Agency (1997), "Interim Guidelines advisory No. 1", Report No. SAC-96-03, SAC Joint Venture, Sacramento, California.
- [8] Goel, S.C., and Stojadinovic, B., and Lee, K.H., Margarian, A.G., Choi, J.H., Wongkaew, A., Reyher, B.P., and Lee, D.Y. (1998), "Conduct Parametric Tests of Unreinforced Connections", Preliminary Report to SAC, Task 7, Subtak 7.02, Unv. of Michigan, Ann Arbor, Michigan.
- [9] Lee, K.H., Goel, S.C., and Stojadinovic, B. (1997), "Boundary Effects in Welded Steel Connections", Report UMCEE 97-20, Dept. of Civ. & Env. Engrg., Unv. of Michigan, Ann Arbor, Michigan.

Biography



Dr. Arnon Wongkaew is a lecturer at Department of Civil Engineering, Faculty of Engineering, Burapha University, Chonburi, Thailand. His research interests are steel structures, finite element analysis, retrofitting and rehabilitation of reinforced concrete structures,

including their applications to the earthquake load.